

AD-A108 022 SRI INTERNATIONAL MEMLO PARK CA F/O 19/1  
STUDY OF FUNDAMENTAL CHEMICAL PROCESSES IN EXPLOSIVE DECOMPOSIT--ETC(U)  
NOV 81 D F MCMLLEN, D M GOLDEN DAA029-78-C-0026  
UNCLASSIFIED SRI-7399 ARO-15501.2-C NL

AD-A108 022 SRI INTERNATIONAL MEMLO PARK CA F/O 19/1  
STUDY OF FUNDAMENTAL CHEMICAL PROCESSES IN EXPLOSIVE DECOMPOSIT--ETC(U)  
NOV 81 D F MCMLLEN, D M GOLDEN DAA029-78-C-0026  
UNCLASSIFIED SRI-7399 ARO-15591.2-C NL

AD-A108 022 SRI INTERNATIONAL MEMLO PARK CA F/O 19/1  
STUDY OF FUNDAMENTAL CHEMICAL PROCESSES IN EXPLOSIVE DECOMPOSIT--ETC(U)  
NOV 81 D F MCMLLEN, D M GOLDEN DAA029-78-C-0026  
UNCLASSIFIED SRI-7399 ARO-15591.2-C NL

AD-A108 022 SRI INTERNATIONAL MEMLO PARK CA F/O 19/1  
STUDY OF FUNDAMENTAL CHEMICAL PROCESSES IN EXPLOSIVE DECOMPOSIT--ETC(U)  
NOV 81 D F MCMLLEN, D M GOLDEN DAA029-78-C-0026  
UNCLASSIFIED SRI-7399 ARO-15591.2-C NL

AD-A108 022 SRI INTERNATIONAL MEMLO PARK CA F/O 19/1  
STUDY OF FUNDAMENTAL CHEMICAL PROCESSES IN EXPLOSIVE DECOMPOSIT--ETC(U)  
NOV 81 D F MCMLLEN, D M GOLDEN DAA029-78-C-0026  
UNCLASSIFIED SRI-7399 ARO-15591.2-C NL

AD-A108 022 SRI INTERNATIONAL MEMLO PARK CA F/O 19/1  
STUDY OF FUNDAMENTAL CHEMICAL PROCESSES IN EXPLOSIVE DECOMPOSIT--ETC(U)  
NOV 81 D F MCMLLEN, D M GOLDEN DAA029-78-C-0026  
UNCLASSIFIED SRI-7399 ARO-15591.2-C NL

AD-A108 022 SRI INTERNATIONAL MEMLO PARK CA F/O 19/1  
STUDY OF FUNDAMENTAL CHEMICAL PROCESSES IN EXPLOSIVE DECOMPOSIT--ETC(U)  
NOV 81 D F MCMLLEN, D M GOLDEN DAA029-78-C-0026  
UNCLASSIFIED SRI-7399 ARO-15591.2-C NL

AD-A108 022 SRI INTERNATIONAL MEMLO PARK CA F/O 19/1  
STUDY OF FUNDAMENTAL CHEMICAL PROCESSES IN EXPLOSIVE DECOMPOSIT--ETC(U)  
NOV 81 D F MCMLLEN, D M GOLDEN DAA029-78-C-0026  
UNCLASSIFIED SRI-7399 ARO-15591.2-C NL

1997, 1998, 1999, 2000, 2001, 2002, 2003, 2004, 2005, 2006, 2007, 2008, 2009, 2010, 2011, 2012, 2013, 2014, 2015, 2016, 2017, 2018, 2019, 2020, 2021, 2022, 2023, 2024, 2025, 2026, 2027, 2028, 2029, 2030, 2031, 2032, 2033, 2034, 2035, 2036, 2037, 2038, 2039, 2040, 2041, 2042, 2043, 2044, 2045, 2046, 2047, 2048, 2049, 2050, 2051, 2052, 2053, 2054, 2055, 2056, 2057, 2058, 2059, 2060, 2061, 2062, 2063, 2064, 2065, 2066, 2067, 2068, 2069, 2070, 2071, 2072, 2073, 2074, 2075, 2076, 2077, 2078, 2079, 2080, 2081, 2082, 2083, 2084, 2085, 2086, 2087, 2088, 2089, 2090, 2091, 2092, 2093, 2094, 2095, 2096, 2097, 2098, 2099, 2100, 2101, 2102, 2103, 2104, 2105, 2106, 2107, 2108, 2109, 2110, 2111, 2112, 2113, 2114, 2115, 2116, 2117, 2118, 2119, 2120, 2121, 2122, 2123, 2124, 2125, 2126, 2127, 2128, 2129, 2130, 2131, 2132, 2133, 2134, 2135, 2136, 2137, 2138, 2139, 2140, 2141, 2142, 2143, 2144, 2145, 2146, 2147, 2148, 2149, 2150, 2151, 2152, 2153, 2154, 2155, 2156, 2157, 2158, 2159, 2160, 2161, 2162, 2163, 2164, 2165, 2166, 2167, 2168, 2169, 2170, 2171, 2172, 2173, 2174, 2175, 2176, 2177, 2178, 2179, 2180, 2181, 2182, 2183, 2184, 2185, 2186, 2187, 2188, 2189, 2190, 2191, 2192, 2193, 2194, 2195, 2196, 2197, 2198, 2199, 2200, 2201, 2202, 2203, 2204, 2205, 2206, 2207, 2208, 2209, 2210, 2211, 2212, 2213, 2214, 2215, 2216, 2217, 2218, 2219, 2220, 2221, 2222, 2223, 2224, 2225, 2226, 2227, 2228, 2229, 2230, 2231, 2232, 2233, 2234, 2235, 2236, 2237, 2238, 2239, 2240, 2241, 2242, 2243, 2244, 2245, 2246, 2247, 2248, 2249, 2250, 2251, 2252, 2253, 2254, 2255, 2256, 2257, 2258, 2259, 2260, 2261, 2262, 2263, 2264, 2265, 2266, 2267, 2268, 2269, 2270, 2271, 2272, 2273, 2274, 2275, 2276, 2277, 2278, 2279, 2280, 2281, 2282, 2283, 2284, 2285, 2286, 2287, 2288, 2289, 2290, 2291, 2292, 2293, 2294, 2295, 2296, 2297, 2298, 2299, 2300, 2301, 2302, 2303, 2304, 2305, 2306, 2307, 2308, 2309, 2310, 2311, 2312, 2313, 2314, 2315, 2316, 2317, 2318, 2319, 2320, 2321, 2322, 2323, 2324, 2325, 2326, 2327, 2328, 2329, 2330, 2331, 2332, 2333, 2334, 2335, 2336, 2337, 2338, 2339, 2340, 2341, 2342, 2343, 2344, 2345, 2346, 2347, 2348, 2349, 2350, 2351, 2352, 2353, 2354, 2355, 2356, 2357, 2358, 2359, 2360, 2361, 2362, 2363, 2364, 2365, 2366, 2367, 2368, 2369, 2370, 2371, 2372, 2373, 2374, 2375, 2376, 2377, 2378, 2379, 2380, 2381, 2382, 2383, 2384, 2385, 2386, 2387, 2388, 2389, 2390, 2391, 2392, 2393, 2394, 2395, 2396, 2397, 2398, 2399, 2400, 2401, 2402, 2403, 2404, 2405, 2406, 2407, 2408, 2409, 2410, 2411, 2412, 2413, 2414, 2415, 2416, 2417, 2418, 2419, 2420, 2421, 2422, 2423, 2424, 2425, 2426, 2427, 2428, 2429, 2430, 2431, 2432, 2433, 2434, 2435, 2436, 2437, 2438, 2439, 2440, 2441, 2442, 2443, 2444, 2445, 2446, 2447, 2448, 2449, 2450, 2451, 2452, 2453, 2454, 2455, 2456, 2457, 2458, 2459, 2460, 2461, 2462, 2463, 2464, 2465, 2466, 2467, 2468, 2469, 2470, 2471, 2472, 2473, 2474, 2475, 2476, 2477, 2478, 2479, 2480, 2481, 2482, 2483, 2484, 2485, 2486, 2487, 2488, 2489, 2490, 2491, 2492, 2493, 2494, 2495, 2496, 2497, 2498, 2499, 2500, 2501, 2502, 2503, 2504, 2505, 2506, 2507, 2508, 2509, 2510, 2511, 2512, 2513, 2514, 2515, 2516, 2517, 2518, 2519, 2520, 2521, 2522, 2523, 2524, 2525, 2526, 2527, 2528, 2529, 2530, 2531, 2532, 2533, 2534, 2535, 2536, 2537, 2538, 2539, 2540, 2541, 2542, 2543, 2544, 2545, 2546, 2547, 2548, 2549, 2550, 2551, 2552, 2553, 2554, 2555, 2556, 2557, 2558, 2559, 2560, 2561, 2562, 2563, 2564, 2565, 2566, 2567, 2568, 2569, 2570, 2571, 2572, 2573, 2574, 2575, 2576, 2577, 2578, 2579, 2580, 2581, 2582, 2583, 2584, 2585, 2586, 2587, 2588, 2589, 2590, 2591, 2592, 2593, 2594, 2595, 2596, 2597, 2598, 2599, 2600, 2601, 2602, 2603, 2604, 2605, 2606, 2607, 2608, 2609, 2610, 2611, 2612, 2613, 2614, 2615, 2616, 2617, 2618, 2619, 2620, 2621, 2622, 2623, 2624, 2625, 2626, 2627, 2628, 2629, 2630, 2631, 2632, 2633, 2634, 2635, 2636, 2637, 2638, 2639, 2640, 2641, 2642, 2643, 2644, 2645, 2646, 2647, 2648, 2649, 2650, 2651, 2652, 2653, 2654, 2655, 2656, 2657, 2658, 2659, 2660, 2661, 2662, 2663, 2664, 2665, 2666, 2667, 2668, 2669, 2670, 2671, 2672, 2673, 2674, 2675, 2676, 2677, 2678, 26

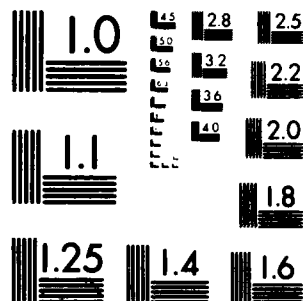
1. **Introduction**

DATE \_\_\_\_\_

97

1. **উদ্দেশ্য**

DTIC



MICROCOPY RESOLUTION TEST CHART  
NATIONAL BUREAU OF STANDARDS 1963-A

LEVEL *11*

ARO 15591.2-C  
*(12)*

November 12, 1981

Final Report *1* *1978* *31 Aug*  
Covering Period ~~20 July 1980~~ to ~~20 July~~ 1981

STUDY OF FUNDAMENTAL CHEMICAL PROCESSES  
IN EXPLOSIVE DECOMPOSITION BY LASER-POWERED  
HOMOGENEOUS PYROLYSIS

By: Donald F. McMillen and David M. Golden

Prepared for:

ARMY RESEARCH OFFICE  
U.S. DEPARTMENT OF THE ARMY  
P.O. Box 1221  
Research Triangle Park, NC 27709

Attention: Dr. Robert Ghirardelli, Director  
Chemical and Biological Sciences

Contract No. DAAG29-78-R-0026  
SRI Project No. 7399

Approved:

*M. E. Hill*  
M. E. Hill, Laboratory Director  
Chemistry Laboratory

G. R. Abrahamson, Vice President  
Physical Sciences Division

DTIC  
DEC 1 1981  
H

DEPT. OF THE ARMY  
SRI PROJECT 7399  
NOV 12 1981

AD A108022  
SRI International



333 Ravenswood Ave. • Menlo Park, California 94025  
(415) 326-6200 • Cable: SRI INTL MPK • TWX: 910-373-1246

81 11 30 079

UNCLASSIFIED

SECURITY CLASSIFICATION OF THIS PAGE (When Data Entered)

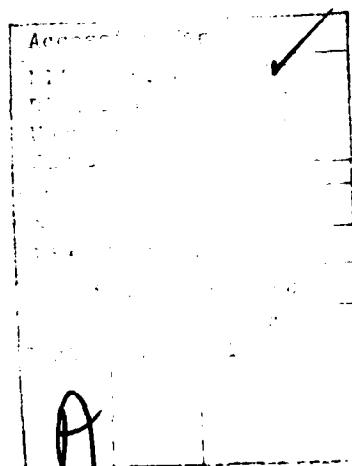
REPORT DOCUMENTATION PAGE		READ INSTRUCTIONS BEFORE COMPLETING FORM
1. REPORT NUMBER	2. GOVT ACCESSION NO.	3. RECIPIENT'S CATALOG NUMBER
	AD-A408021	
4. TITLE (and Subtitle)	5. TYPE OF REPORT & PERIOD COVERED	
STUDY OF FUNDAMENTAL CHEMICAL PROCESSES IN EXPLOSIVE DECOMPOSITION BY LASER-POWERED HOMOGENEOUS PYROLYSIS	FINAL Covering Period 20 July 1980 to 30 July 1981	
7. AUTHOR(s)	6. PERFORMING ORG. REPORT NUMBER	
Donald F. McMillen and David M. Golden	7399	
9. PERFORMING ORGANIZATION NAME AND ADDRESS	8. CONTRACT OR GRANT NUMBER(s)	
SRI International 333 Ravenswood Avenue Menlo Park, CA 94025	DAAG29-78-D-0026 C	
11. CONTROLLING OFFICE NAME AND ADDRESS	10. PROGRAM ELEMENT, PROJECT, TASK AREA & WORK UNIT NUMBERS	
U. S. Army Research Office Post Office Box 12211 Research Triangle Park, NC 27709	Project PYU 7399	
14. MONITORING AGENCY NAME & ADDRESS (if different from Controlling Office)	12. REPORT DATE	
	12 November 1981 (12) 6+	
	13. NUMBER OF PAGES	
	12 + 46 (appendices) = 58	
	15. SECURITY CLASS. (of this report)	
	Unclassified	
	15a. DECLASSIFICATION/DOWNGRADING SCHEDULE	
16. DISTRIBUTION STATEMENT (of this Report)		
Approved for public release; distribution unlimited.		
17. DISTRIBUTION STATEMENT (of the abstract entered in Block 20, if different from Report)		
NA		
18. SUPPLEMENTARY NOTES		
The view, opinions, and/or findings contained in this report are those of the author(s) and should not be construed as an official Department of the Army position, policy, or decision, unless so designated by other documentation.		
19. KEY WORDS (Continue on reverse side if necessary and identify by block number)		
20. ABSTRACT (Continue on reverse side if necessary and identify by block number)		
See next page.		

# ABSTRACT

Very Low-Pressure Pyrolysis studies of 2,4-dinitrotoluene [K S]  
decomposition resulted in decomposition rates consistent with  $\log [k/s^{-1}] =$   
12.1 - 43.9/2.3 RT. These results support the conclusion that previously  
reported "anomalously" low Arrhenius parameters for the homogeneous gas-  
phase decomposition of ortho-nitrotoluenes actually represent surface-  
catalyzed reactions. Preliminary qualitative results for pyrolysis of  
ortho-nitrotoluene in the absence of hot reactor walls, using the Laser-  
Powered Homogeneous Pyrolysis technique (LPHP), provide further support for  
this conclusion: only products resulting from Ph-NO<sub>2</sub> bond scission were  
observed; no products indicating complex intramolecular oxidation-reduction  
or elimination processes could be detected. The LPHP technique was  
successfully modified to use a pulsed laser and a heated flow system, so  
that the technique becomes suitable for study of surface-sensitive, low  
vapor pressure substrates such as TNT. The validity and accuracy of the  
technique was demonstrated by applying it to the decomposition of  
substances whose Arrhenius parameters for decomposition were already well  
known. IR-fluorescence measurements show that the temperature-space-time  
behavior under the present LPHP conditions is in agreement with  
expectations and with requirements which must be met if the method is to  
have quantitative validity. LPHP studies of azoisopropane decomposition,  
chosen as a radical-forming test reaction, show the accepted literature  
parameters to be substantially in error and indicate that the correct  
values are in all probability much closer to those measured in this work:  
 $\log [k/s^{-1}] = 13.9 - 41.2/2.3 RT.$

## CONTENTS

ABSTRACT . . . . .	11
INTRODUCTION.. . . .	1
SUMMARY OF RESULTS.. . . .	3
VERY LOW-PRESSURE PYROLYSIS OF 2,4-DINITROTOLUENE. . . . .	5
REFERENCES . . . . .	12
APPENDIX A: Laser-Powered Homogeneous Pyrolysis of Aromatic Nitro Compounds	
APPENDIX B: Laser-Powered Homogeneous Pyrolysis: Thermal Studies under Homogeneous Conditions, Validation of the Technique and Application to the Mechanism of Azo-Compound Decomposition	



## INTRODUCTION

This report describes the results of a study whose ultimate objective is to elucidate the nature of the initial chemical steps in the gas-phase homogeneous decomposition of 2,4,6-trinitrotoluene and other nitroaromatics. The specific objectives for the phase of the work reported here were to adapt LPHP for use with a pulsed laser and a heated flow system so that the requirements imposed by low vapor pressure, surface-sensitive, radical-forming substrates could be met. This specific objective included the measurement of temperature in the laser-heated zone by spectroscopic and chemical techniques as a function of a number of variables, in order to ascertain whether molecules used as substrates and temperature standards reach the same temperature for the same time, and whether this temperature is sufficiently constant as a function of time and space to ensure accurate and precise measurement of Arrhenius parameters for thermal decomposition. As the report describes, the specific objectives have been fully achieved. This means that, although the ultimate objective of elucidating the homogeneous gas-phase decomposition chemistry of TNT has not yet been fully reached in this work, the technique necessary to do so has been developed and tested.

During the same period, progress has been made by other researchers in understanding certain aspects of TNT decomposition, but the difficulties adhering to the general decomposition behavior of explosives and to the particular characteristics of TNT have prevented answering, by any technique, the particular questions addressed by this work. Thus, knowledge of the chemical behavior of isolated gas-phase TNT molecules as a basis for understanding not only how, but also why, TNT behaves as it does during condensed-phase decomposition has yet to be obtained.



## SUMMARY OF RESULTS

The results of this work are described, in significant part, in two papers: one published in the Journal of Physical Chemistry and one just accepted by that journal. These papers, as Appendices A and B, respectively, constitute the major part of this report. The body of the report is limited to a summary of the results reported in the two papers and a description of other results not included in them. The work and conclusions reached, as described in the next section and in the appendices, include the following:

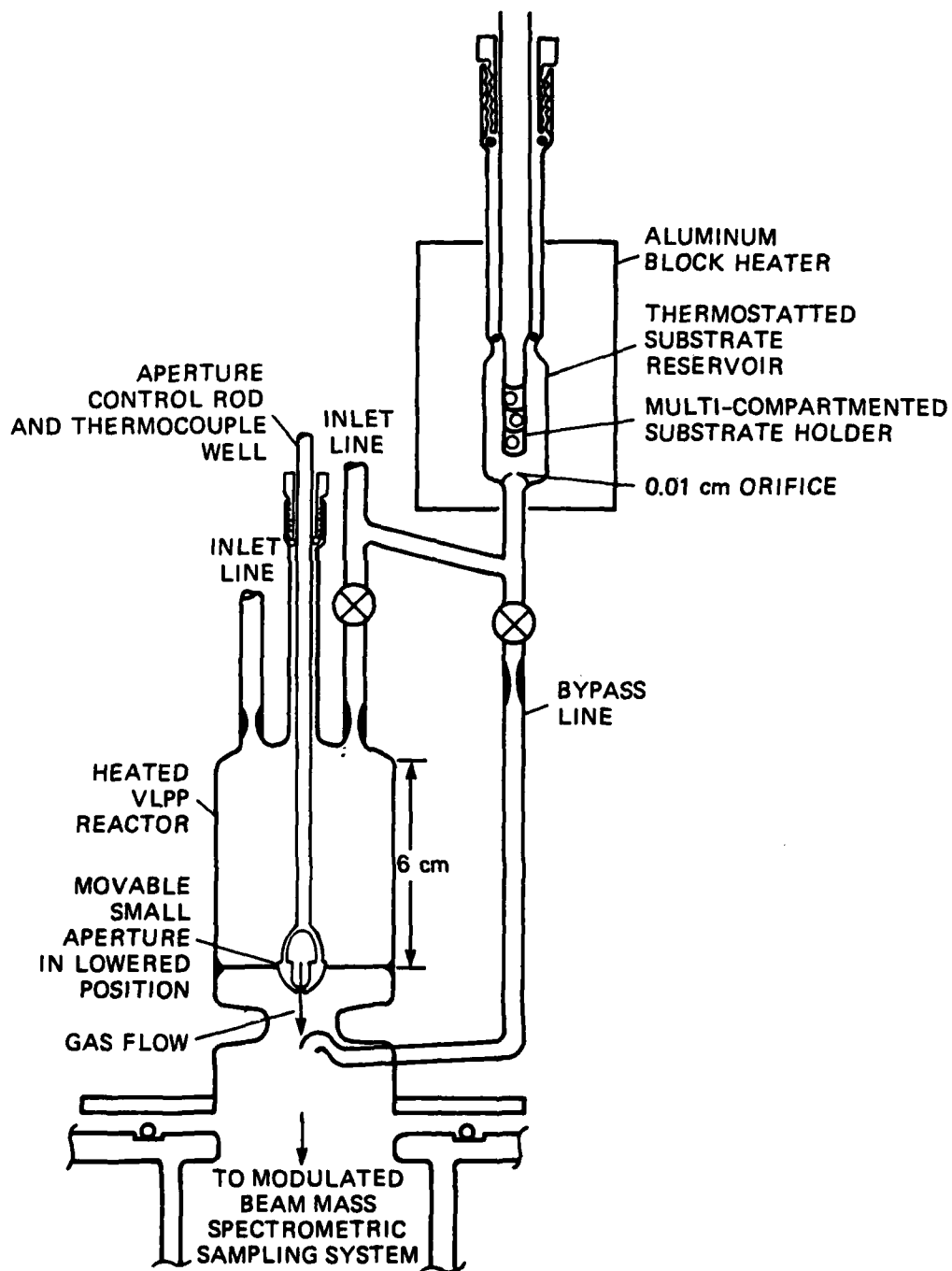
- (1) Confirmation through Very Low-Pressure Pyrolysis (VLPP) studies that the low temperature, "gas-phase" rate parameters previously reported for ortho-nitrotoluenes<sup>1</sup> are real: the "low" Arrhenius parameters almost certainly are not caused either by systematic errors or by rate control exerted by secondary reactions.
- (2) Support from these VLPP studies for the conclusion that some previous kinetic studies of ortho-nitrotoluene decomposition in which intramolecular oxidation-reduction processes were observed under nominal gas-phase conditions had, in all probability, provided conditions where reaction was primarily by surface-catalyzed reactions.
- (3) Preliminary qualitative evidence from the LPHP technique (static system) that no intramolecular oxidation-reduction products are formed when the decomposition of ortho-nitrotoluene is carried out under conditions where there can be no catalysis of decomposition by hot reactor walls.
- (4) Successful modification of the LPHP technique to use a pulsed laser and a flow system, making the method suitable for study of surface-sensitive, low vapor pressure substances such as TNT.

- (5) Successful LPHP reproduction of well-documented Arrhenius parameters for "test" substrates which decompose by straightforward molecular elimination reactions. This demonstrates that:
- (a) Temperature accommodation is sufficiently rapid and equal for different substrates that they reach the same temperature for the same time period.
  - (b) The comparative-rate technique for measuring the temperature dependence of reaction rates is so successful at accommodating the temperature-space-time inhomogeneities known to exist under the laser heating conditions that the activation parameters can be measured with no more than a few percent error.
- (6) Demonstration by IR-fluorescence measurements that (1) the LPHP temperature-space-time behavior is in qualitative agreement with general expectations and in fair quantitative agreement with acoustic wave calculations performed for a simplified model, and (2) that temperature-space-time inhomogeneities can readily be made less significant than variations which can be accommodated by the comparative-rate technique used in this modification of LPHP.
- (7) Demonstration, through a study of azoisopropane decomposition, that the currently used, gas-chromatographically monitored, flow system LPHP technique is suitable also for the more difficult case of radical-forming reactions. This study (1) revealed that the Arrhenius parameters "accepted" in the literature for the azoisopropane test substrate<sup>2</sup> were substantially in error and (2) served to reconcile classes of kinetic data for this substrate that were previously incompatible.

## VERY LOW-PRESSURE PYROLYSIS OF 2,4-DINITROTOLUENE

In addition to work performed as described in the appendices, we obtained the following results from Very Low-Pressure Pyrolysis studies of 2,4-dinitrotoluene decomposition. In brief, these results indicated that surface-catalyzed reactions were, in this case, unavoidable under the higher gas-wall collision frequency conditions of VLPP. They also supported, but did not prove, our previous speculation that the low Arrhenius parameters and "anomalous" products which had been reported for the gas-phase decomposition of ortho-nitrotoluene (including TNT) were really caused by surface-catalyzed reactions. These results, discussed below in more detail, led to our choice of Laser-Powered Homogeneous Pyrolysis<sup>3</sup> as an attractive method for studying the homogeneous gas-phase decomposition of nitroaromatics and other surface-sensitive substrates under conditions where there is no contact between substrate molecules and hot reactor walls. The use of LPHP in a static system for qualitative studies of nitrobenzene and ortho-nitrotoluene decomposition, and the subsequent modification of LPHP which utilizes a pulsed laser and a heated flow system and is thereby suitable for use with low vapor pressure substrates, are described in detail in Appendices A and B.

The vapor-phase decomposition of 2,4-dinitrotoluene (DNT) was studied in a VLPP system equipped with a heated inlet line and a variable aperture reactor very similar to the one shown in Figure 1. This technique has been described in detail previously.<sup>4</sup> Its principal advantage for study of the initial steps of complex decomposition processes is that at very low pressures most products formed in initial decomposition steps will escape

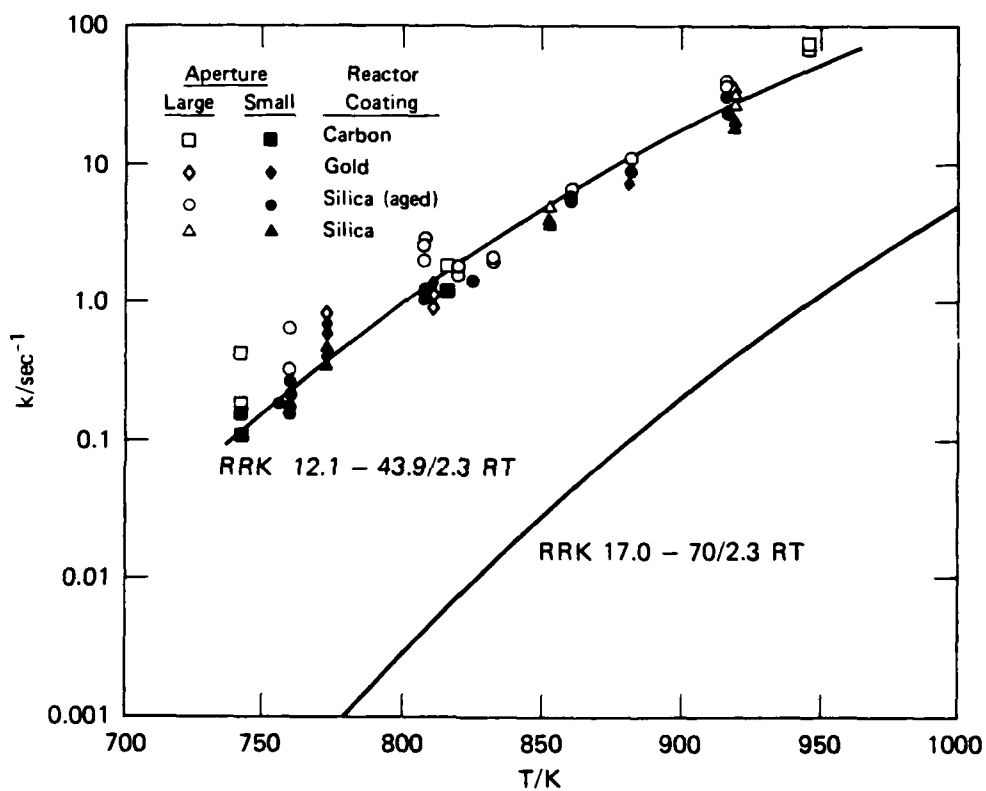


SA-4799-45AR

FIGURE 1 VARIABLE APERTURE VERY LOW-PRESSURE PYROLYSIS REACTOR

from the reactor to the detection system before they undergo many gas-gas collisions and thus before they have any chance to undergo secondary reactions. Furthermore, the molecular-beam, mass spectrometric detection system generally enables identification of initial products (e.g., radicals) under conditions where they make no collisions with, and therefore undergo no secondary reactions on, the metal walls of the mass spectrometer chamber. As will be seen below, while these are indeed advantages of the VLPP method, they are useful for studying homogeneous decomposition processes only when heterogeneous (i.e., surface-catalyzed) reactions in the heated reactor can be avoided.

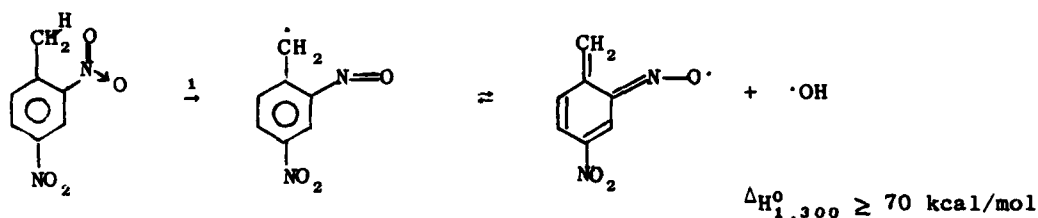
Figure 2 shows the measured rates of dinitrotoluene decomposition as a function of temperature with four different reactor wall coatings. The solid lines represent rates corresponding to the sets of "high" and "low" Arrhenius parameters indicated in the figure, where the extent of fall-off has been estimated by the RRK procedure.<sup>5</sup> The data are consistent with the rate parameters  $\log k/\text{sec}^{-1} = 12.1 - 43.9/2.3 RT$ , but are clearly not consistent with  $\log k = 17.0 - 70/2.3 T$ , values which would have been indicative of unimolecular scission of the  $\text{Ph-NO}_2$  bond.<sup>6</sup> Within the scatter of the data, changing the reactor surface from a "normally aged" to a freshly cleaned ( $\text{O}_2$  at  $800^\circ\text{C}$  for 2 hours), to an intentionally carbon-coated (1,5-hexadiene pyrolysis at  $850^\circ\text{C}$ ), or to a gold-coated surface, has little effect. Although the observation of similar reaction rates for different surfaces is often taken as evidence that surface-catalyzed reactions are unimportant, that conclusion does not appear to be justified in this case. In the first place, an A-factor of  $10^{12.1} \text{ sec}^{-1}$  and an



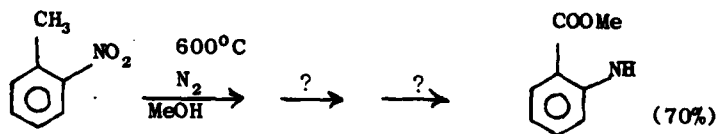
JA-322522-11

FIGURE 2 VERY LOW-PRESSURE PYROLYSIS OF 2,4-DINITROTOLUENE

activation energy of 44 kcal/mol, which are quite consistent with the ca. 12.4 and 48 values that other workers have reported for ortho-substituted nitrotoluenes, cannot be associated with any plausible homogeneous gas-phase reaction for dinitrotoluene. For example, the hydroxyl radical elimination suggested by Matveev, among others, is far too endothermic to account for the observed activation energy,<sup>6b</sup> even assuming the nitrosobenzyl radical exhibits an unlikely additional 10 kcal/mol resonance stabilization over that shown by benzyl radical itself.



The more thermodynamically favored products which have actually been recovered as ultimate products<sup>7</sup> require a degree of molecular rearrangement--transfer of two hydrogens to nitrogen and two oxygens to carbon--that is without precedent as a fundamental chemical step for an isolated reactant molecule.<sup>8</sup>



Furthermore, a rough mass balance shows that only ~20% of the DNT decomposed exits the reactor to the detection system, the remainder evidently being deposited on the reactor surface. In other words, some

surface reactions are clearly very important, and it is likely that the initial decomposition step is among these. Also, rapid deposition of decomposition products on the reactor surface could explain why the behavior was similar with all types of surface preparation: the character of the surface quickly became that of DNT products, no matter what coating had been initially deposited.

Thus, all indications are that in the decomposition of 2,4-dinitrotoluene the high gas-wall collision frequency of VLPP and the proclivity of DNT for surface-catalyzed reactions make the VLPP method unsuitable for studying homogeneous gas-phase processes of this or similar substrates. This is in contrast to many other substrates where surface contributions were either not observed at all or could be satisfactorily suppressed with the appropriate reactor-surface treatments.<sup>4</sup> The similarity of the parameters observed here and those reported by other workers<sup>1</sup> for reaction under nominal homogeneous gas-phase conditions further supports our conclusion that there, too, surface-catalyzed reactions were important.

Although a technique such as VLPP might ultimately be used purposely to study wall-catalyzed processes of DNT, TNT, or similar substrates, our present objective is to learn about the behavior of isolated DNT and TNT molecules, in order to establish a base of information on which an improved understanding of the behavior of TNT in contact with solid surfaces and in condensed phases can be developed. These initial experiments made it obvious that if the use of low substrate partial pressure as a means of eliminating secondary reactions were to be the basis of a viable technique for studying the homogeneous gas-phase reactions of nitrotoluenes, it was



necessary to eliminate or greatly reduce gas-wall collisions. Clearly, it was desirable to maintain a low substrate partial pressure, but it was also necessary to raise the total pressure (for example, by dilution in an inert gas) and to heat the substrate by other means than contact with hot walls.

Among the possible ways to meet these requirements, one of those most adaptable to low-vapor pressure substrates appeared to be rapid heating by an infrared laser. Appendices A and B describe such a technique, Laser-Powered Homogeneous Pyrolysis (LPHP).<sup>3</sup> Also described are (1) the results of preliminary, qualitative experiments with nitroaromatics using this technique, (2) the modification of the technique to meet the requirements for precise determination of rate parameters as imposed by low vapor pressure, surface-sensitive, radical-forming substrates, and (3) the demonstration of the validity and accuracy of the technique, using radical-forming and molecular elimination substrates with known Arrhenius parameters. Thus, appendices A and B describe the development and testing of a technique that provides the capabilities necessary for elucidation of the homogeneous gas-phase decomposition chemistry of TNT and other energetic materials.

# REFERENCES

1. V. G. Matveev, V. V. Dubikhin, and G. M. Nazin, Inst. Khim. Fiz, Cheronogolovka, USSR 4 783 (1978) and Acad. Sci. USSR Bull., Div. Chem. Sci. 2, 474 (1978), and references cited therein; Y. Y. Maksimov, Russ. J. Phys. Chem., 46, 990 (1972), or Dubovitskii, et al., ibid. 35 148 (1961); Y. Y. Maksimov and L. T. Pavlik, Russ. J. Phys. Chem. 49, 360 (1975).
2. P. S. Engel, Chem. Rev. 80, 99 (1980); M. J. Perona, P. C. Beadle, and D. M. Golden, Int. J. Chem. Kinetics, 5, 495 (1973).
3. W. M. Shaub and S. H. Bauer, Int. J. Chem. Kinetics, 7, 509 (1975); W. M. Shaub, Ph.D. Thesis, Cornell University (1975).
4. D. M. Golden, G. N. Spokes, and S. W. Benson, Angew. Chem. (Int'l ed.) 12, 534 (1973); M. Rossi, K. D. King, and D. M. Golden, J. Amer. Chem. Soc., 101, 1223 (1979).
5. G. Emanuel, Int. J. Chem. Kinetics, 4, 591 (1972).
6. D. R. Stull, E. P. Westrum, Jr., and G. C. Sinke, The Chemical Thermodynamics of Organic Compounds, John Wiley and Sons, Inc., New York (1969), p. 672; S. W. Benson, Thermochemistry and Chemical Kinetics, 2nd ed., John Wiley and Sons, Inc., New York (1976).
7. E. K. Fields and S. Meyerson, "Formation and Reactions of Free Radicals from Pyrolysis of Nitro Compounds," in Advances in Free Radical Chemistry, 5, 101 (1965); E. K. Fields, Tetrahedron Letters, 10, 1201 (1968).
8. S. W. Benson and H. E. O'Neal, Kinetic Data on Gas-Phase Unimolecular Reactions, National Standard Reference Data System, NSRDS-NBS-21, 1970.

Appendix A

LASER-POWERED HOMOGENEOUS PYROLYSIS  
OF AROMATIC NITRO COMPOUNDS

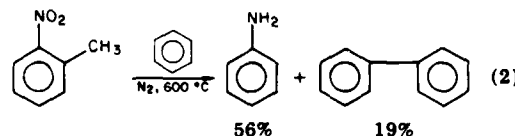
### Laser-Powered Homogeneous Pyrolysis of Aromatic Nitro Compounds

Publication costs assisted by the Army Research Office

**Sir:** Recently the use of a CW infrared laser to provide a fully equilibrated, internally heated, isothermal reaction technique called laser-powered homogeneous pyrolysis (LPHP) has been successfully demonstrated on a number of low-molecular-weight model substrates.<sup>1</sup> This technique utilizes an unreactive bath gas to absorb the infrared radiation and to transfer this energy by collision with the substrate. The pressures are maintained sufficiently high (typically 50–100 torr), such that thermal distribution of energy takes place faster than chemical reaction, and multiphoton decomposition is avoided. We report the application of a variation of this technique to a type of substrate for which surface-catalyzed reactions are so facile that gas-phase decomposition, which was demonstrably free from surface contributions, has not been previously reported.<sup>2</sup> The results of initial, qualitative experiments indicate that reactions previously thought to have been carried out under conditions which precluded surface-catalyzed reactions<sup>2</sup> were, in fact, largely heterogeneous.

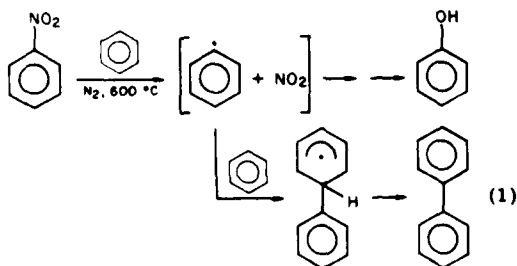
Sometime ago, Fields and Meyerson reported<sup>3</sup> that nitrobenzene pyrolyzed in a packed reactor in a N<sub>2</sub> carrier containing excess benzene provided products correspond-

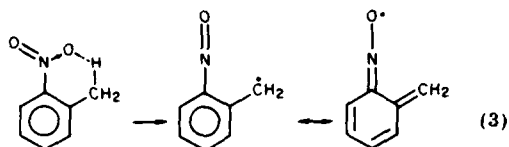
ing to simple cleavage of the weakest bond in the molecule and thus expected under homogeneous conditions (eq 1). On the other hand, the reaction of *o*-nitrotoluene under the same conditions provided only minor amounts of biphenyl, with the principal product being aniline (eq 2).<sup>3</sup>



These results led the authors to suggest that reaction of the ortho-substituted nitrobenzene took place by way of a cyclic transition state. Similarly, Matveev and co-workers<sup>4</sup> have determined Arrhenius parameters for the homogeneous gas-phase decomposition of nitrobenzene and meta- and para-substituted nitrobenzenes which are consistent with simple cleavage of the phenyl-NO<sub>2</sub> bond, that is, generally having Arrhenius activation energies of  $70 \pm 3$  kcal/mol and A factors of  $10^{17.0 \pm 0.5} \text{ s}^{-1}$ . However, for *o*-methyl-substituted nitrobenzenes, the observed decomposition rates provided substantially lower Arrhenius parameters. In the case of *o*-nitrotoluene, they report<sup>2</sup>  $E = 49.5 \pm 1.3$  kcal/mol and  $A = 10^{12.4 \pm 0.4} \text{ s}^{-1}$ .

Since these parameters were determined under conditions<sup>2,4</sup> which for the meta and para isomers were sufficient to totally eliminate surface-catalyzed reactions, the authors came to the conclusion that the lowered Arrhenius parameters reflect gas-phase homogeneous decomposition by way of a cyclic transition state and suggested that the initial step is cyclic elimination of OH to produce a substituted benzyl radical (eq 3). Although such a step is plausible on steric grounds, the estimated<sup>5</sup> endothermicity of  $70 \pm 7$  kcal/mol, plus an intrinsic activation energy of at least 20 kcal/mol, eliminate this sequence from consideration as an important homogeneous gas-phase process, let alone as one providing an Arrhenius activation energy of less than 50 kcal/mol. The net reaction (to aniline and





$\text{CO}_2$ ) is substantially more favored<sup>5</sup> ( $\Delta H^\circ_{298} \approx -82$  kcal/mol), but the transfer of four atoms, which is required to produce this end result, seems far too complex to take place as an elementary step. On the other hand, since polynitroaromatics are a class of compounds useful because their decomposition pathways are unlike those of "normal" organic compounds, experimental verification of this conclusion and elucidation of the true mechanism are desirable. Thus, the LPHP technique was used to carry out the decomposition of nitrobenzene and ortho-substituted nitrobenzenes under conditions which preclude all surface reactions.

The pyrolysis cell was Pyrex cylinder 10 cm  $\times$  2.2 cm diameter, fitted with O-ring sealed KCl windows. The infrared absorber was  $\text{SF}_6$ . The partial pressures in the cell were as follows: argon,  $\sim 20$  torr;  $\text{SF}_6$ , 10–20 torr; benzene, 2 torr; and nitrobenzene or o-nitrotoluene,  $\sim 0.2$  torr. The cell was maintained at  $\sim 70^\circ\text{C}$  to prevent condensation of the substrates. The heat source was a home-made pulsed  $\text{CO}_2$  laser, nominally similar to one section of a Lumonics Model 203 laser. When tuned to the 10.57- $\mu\text{m}$ , P(18) line, the laser provided  $\sim 0.5$  J/pulse. In order to bring about significant decomposition, partial focusing of the beam (to  $\sim 1$  cm) was required. With this beam diameter, the fluence was  $\sim 0.6$  J/cm<sup>2</sup>. From the fractional decomposition observed ( $\sim 1$ –4% per flash in the path of the laser beam), and a probable reaction time of  $\sim 20$   $\mu\text{s}$  before cooling by an expansion wave,<sup>6</sup> the reaction temperature can be estimated to be between 1000 and 1200 K. Products were determined by gas chromatographic analysis and by GC-MS.

Pyrolysis of nitrobenzene in the presence of excess benzene yielded biphenyl as the principal product, consistent with the results of Fields and Meyerson.<sup>3</sup> However, pyrolysis of o-nitrotoluene under the same conditions yielded principally biphenyl and methylbiphenyl(s) with no aniline or other products indicative of an internal ox-

idation-reduction reaction. GC-MS analysis would have detected aniline at a level corresponding to  $\leq 1\%$  of the biphenyl yield. Even at a temperature as high as 1200 K, the 70 kcal/mol bond scission process would predominate over the surface-catalyzed, low activation energy process only by a factor of 2 or 3, if the latter were accessible. Thus, a substrate for which heterogeneous reaction had, under all previously reported conditions, been predominant<sup>2</sup> appears to react, under LPHP conditions,  $>99\%$  by a homolytic bond scission process.

We are currently in the process of using chemical and physical (spectroscopic) probes to determine the extent of temperature variation within the laser-heated region as a function of time and space for various combinations of absorber, inert collider gas, and substrate. If, as recent reports might suggest,<sup>6</sup> conditions which minimize these variations are readily accessible, then LPHP operated with a heated flow system in a multiple flash mode will offer the same advantage for decomposition rate studies as the comparative rate shock tube technique, but be applicable to compounds of such low vapor pressure that their study by the shock tube technique is impractical.

#### References and Notes

- (1) W. M. Shaub and S. H. Bauer, *Int. J. Chem. Kinet.*, **7**, 509 (1975); W. M. Shaub, Ph.D. Thesis, Cornell University, 1975.
- (2) V. G. Matveev, V. V. Dubikhin, and G. M. Nazin, *Acad. Sci. USSR. Bull. Div. Chem. Sci.*, No. 2, 474 (1978), and references cited therein.
- (3) (a) E. K. Fields and S. Meyerson, *Tetrahedron Lett.*, **10**, 1201 (1968); (b) E. K. Fields and S. Meyerson, *Adv. Free Radical Chem.*, **5**, 101–187 (1965).
- (4) V. G. Matveev, V. V. Dubikhin, and G. M. Nazin, *Inst. Khim. Fiz. Cherenogolovka, USSR*, No. 4, 783 (1978).
- (5) (a) R. Shaw, *J. Phys. Chem.*, **75**, 4047 (1971); (b) "Handbook of Chemistry and Physics", 49th ed, The Chemical Rubber Co., Cleveland, Ohio, 1968. (c) S. W. Benson, "Thermochemistry and Chemical Kinetics", 2nd ed, Wiley, New York, 1976.
- (6) (a) C. Steel, V. Starov, R. Leo, P. John, and R. G. Harrison, *Chem. Phys. Lett.*, **82**, 121 (1979). (b) D. Guzman, W. Braun, and W. Tsang, *J. Chem. Phys.*, **87**, 4291 (1977); (c) R. N. Zitter and D. F. Koester, *J. Am. Chem. Soc.*, **100**, 2265 (1978); (d) M. H. Back and R. A. Back, *Can. J. Chem.*, **57**, 1511 (1979); (e) E. Grunwald, C. M. Lonsetta, and S. Popek, *J. Am. Chem. Soc.*, **101**, 5063 (1979).

Chemical Kinetics Department  
SRI International  
Menlo Park, California 94025

K. E. Lewis  
D. F. McMillen\*  
D. M. Golden

Received October 29, 1979

Appendix B

LASER-POWERED HOMOGENEOUS PYROLYSIS:  
THERMAL STUDIES UNDER HOMOGENEOUS CONDITIONS,  
VALIDATION OF THE TECHNIQUE AND APPLICATION TO  
THE MECHANISM OF AZO-COMPOUND DECOMPOSITION

Submitted to  
J. Phys. Chem.  
(sp.issue--Bauer)

LASER-POWERED HOMOGENEOUS PYROLYSIS:  
THERMAL STUDIES UNDER HOMOGENEOUS CONDITIONS,  
VALIDATION OF THE TECHNIQUE AND APPLICATION TO  
THE MECHANISM OF AZO-COMPOUND DECOMPOSITION

D. F. McMillen, K. E. Lewis, G. P. Smith, and D. M. Golden  
Department of Chemical Kinetics  
SRI International, Menlo Park, CA 94025

ABSTRACT

An infrared laser is used as a "thermal switch" to study pyrolysis reactions under effectively wall-less conditions. The technique has been substantiated with both chemical (known rate constants) and physical (observation of infrared fluorescence from bath gases) calibrations.

Accepted values for Arrhenius parameters for the decomposition of isobutyl bromide, isopropyl acetate, and ethyl acetate have been reproduced. The decomposition of 2,2'-azoisopropane is determined to be best represented by the expression  $\log [k/s^{-1}] = 13.9 - 41.2/\theta$ ;  $\theta = 2.303 RT/\text{kcal mole}^{-1}$ . This suggests a concerted pathway for the decomposition, in contrast to some previous findings.

## I INTRODUCTION

The utility of various types of lasers as a means of rapidly and selectively exciting substrate molecules is well recognized and has been widely exploited in recent years. Many studies of energy transfer and disposition, and the resulting chemical reactions, which were not before possible, have now been published.<sup>1</sup> However, relatively little effort seems to have been spent on the use of lasers as heat sources in the parameterization of normal "thermal" chemical reactions.<sup>2a-f</sup> One such application where infrared lasers could prove extremely valuable is in the determination of activation parameters for the decomposition of molecules where the traditional heating by a hot-walled vessel is inappropriate because of surface sensitivity, and where the use of shock-tube techniques is made difficult by low substrate volatility.

We describe here a technique which will enable such parameterizations to be made precisely and on a routine basis. This technique, called Laser-Powered-Homogeneous-Pyrolysis (LPHP) is a modification of the technique first described by Shaub and Bauer<sup>2a</sup> in which an infrared laser is used to heat an absorbing, but unreactive, gas which then collisionally transfers its energy to the reactive substrate. Under these conditions, there is no surface component to the substrate reaction, since the walls remain cold relative to the reaction temperature. Furthermore, the need to explicitly and precisely define a reaction temperature is eliminated by use of an internal standard, a substrate whose Arrhenius parameters are well known, in a procedure exactly analogous to the comparative rate single-pulse shock-tube technique.<sup>3</sup> The technique described by Shaub and Bauer<sup>2a-b</sup> utilized a cw laser and a static cell to determine the Arrhenius parameters for a number of high vapor pressure substrates which undergo



molecular elimination reactions. The measured parameters agreed within an average of 6% with previously reported values.

The modification of the method described here incorporates a (moderately) heated flow system and a pulsed-infrared laser (Lumonics K-103). The heated flow system makes the technique suitable for study of substrates having room temperature vapor pressures as low as  $\sim 10^{-5}$  torr. The use of a laser which is repeatedly pulsed for very short periods and the rapid expansion wave cooling which takes place after each pulse facilitates the operation of a flow system under "steady state" conditions with relatively high reaction temperatures. Steady state refers to the balance between replenishment and decomposition. These conditions in turn help to minimize secondary reactions. The technique was applied to the study of three molecular elimination processes and a radical-forming reaction. In the case of the molecular elimination processes, the previously reported parameters have been reproduced; for azoisopropane (AIP) pyrolysis, the previously "accepted" parameters can now be seen to be substantially in error, and the current results add new insight to the classic problem of the mechanism azoalkane decomposition.

## II DESCRIPTION OF THE TECHNIQUE

Figure 1 shows a schematic of the LPHP flow system. Typically, a mixture of  $\text{SF}_6$  (infrared absorber),  $\text{CO}_2$  (inert collider), temperature standard (e.g., t-butyl acetate), and substrate flows from a storage bulb through a flow-controlling valve, through parallel temperature-controlled reservoirs where split streams of this mixture are saturated with scavenger and substrate (if the substrate has a low vapor pressure). The gas mixture then flows through the reaction cell, a gas-chromatograph

sampling valve, a second needle valve, and into a vacuum pump. Total pressure is maintained at the desired level by adjustment of the second needle valve.

In operation, flow is maintained at a constant level until steady state is reached, and then the laser is fired at a constant repetition rate (typically, 0.25 Hz) until a new steady state of product(s) and undecomposed substrate is attained. The duration of the laser pulse is  $\sim 1 \mu\text{sec}$ ; substrate heating takes place within 1-3 microseconds following this pulse (see below), and decomposition continues for the next 5-10  $\mu\text{sec}$  until the gas mixture is cooled by expansion behind a compression wave which moves radially outward at near-sonic velocity. The details of this heating and cooling are discussed below; it is clear, however, that the general behavior is illustrated by Figure 2, a schematic representation of the spatially-averaged substrate concentration as a function of time. The type of concentration-time behavior shown in Figure 2 presents the choice of measuring either the local concentration within the laser-heated region on a real-time basis, or the average cell concentration on a time-averaged basis. In all of the experiments described here, the average concentration was measured gas chromatographically (FID) primarily because the easily accessible, very wide dynamic range of gc enables precise measurements to be made over a wide range of fractional decomposition. (In ongoing and future work, we are combining the capability for making measurements of average concentration with molecular beam extraction and real-time mass spectrometric detection of products, as well as real-time in situ optical detection using laser-induced fluorescence.)

On inspection of Figure 2, it is obvious that the maximum information can be obtained from measurements of average concentration when the rapid drop in concentration following any individual laser shot is small compared

to the overall change between laser-off and laser-on "steady state" conditions. This is accomplished by adjusting conditions so that the fractional decomposition (in the heated volume) per laser shot is small, and so that there are a significant number (e.g., 25) of laser shots during the average flow lifetime of a substrate molecule in the reaction cell. Under these conditions, the algebraic analysis is simplified if complete mixing of the heated and unheated regions takes place between laser shots. The toroidally-shaped reaction cell, shown in Figure 1, was designed so that diffusional processes would ensure that the latter criterion is met.

Under the pseudo-steady-state conditions described above and illustrated in the right-hand portion of Figure 2, the decrease in average concentration of substrate A during any single laser shot equals the replenishment (by flow) of A before the next laser shot. This results, as shown in Appendix A, in equation (1):

$$k\tau_r \cong -\ln \left[ 1 - \left( \frac{A_0}{A_{ss}} - 1 \right) \frac{V_T}{V_R} \left( \frac{\tau_L}{\tau_F} \right) \right] \quad (1)$$

where  $k$  is the first-order rate constant describing disappearance of A,  $\tau_r$  is the reaction time (ca. 10  $\mu$ sec) following each laser pulse,  $\tau_L$  is time between laser pulses (typically 4 sec),  $\tau_F$  is the flow lifetime in the reaction cell (typically 200 sec),  $V_T$  and  $V_R$  are the total and laser-heated cell volumes, respectively, and  $A_0$  and  $A_{ss}$  are, as indicated in Figure 2, the laser-off and laser-on steady state substrate concentrations, respectively.

The need to measure explicitly the temperature corresponding to any particular measurement of  $k$  is eliminated by concurrent determination of the fractional decomposition of a temperature standard, a substrate whose

Arrhenius parameters are already well known. According to equation (2),

$$\log k_1 \tau_r = \log A_1 - \left(1 - \frac{E_1}{E_2}\right) \log \tau_r - \frac{E_1}{E_2} \log A_2 + \frac{E_1}{E_2} \log k_2 \tau_r \quad (2)$$

a plot of  $\log k_1 \tau_r$  versus  $\log k_2 \tau_r$  gives a straight line of slope  $E_1/E_2$  and an intercept of  $\log A_1 - \left(1 - \frac{E_1}{E_2}\right) \log \tau_r - \frac{E_1}{E_2} \log A_2$ . This approach has been extensively exploited in the comparative rate single-pulse shock-tube technique as developed by Tsang,<sup>3</sup> and commonly results in measurements of activation energies with random errors of  $\leq 0.3$  kcal/mole. Inspection of equation (2) reveals that uncertainties in reaction time,  $\tau_r$ , will cause no error in the slope of the comparative rate plot (the measured activation energy) and that the error in the intercept (A-factor) will be given by  $(1 - E_1/E_2) \log \frac{\tau_r \text{ true}}{\tau_r \text{ est.}}$ . When  $E_1$  and  $E_2$  are not greatly different, this error will be insignificant. For example, when  $E_1/E_2 = 0.9$ , even a ten-fold error in  $\tau_r$  will result in an error in  $\log A_{\text{meas}}$  of only 0.1 log units.

### III PHYSICS OF THE PULSED-LASER PYROLYSIS PROCESS

To design experiments properly and to utilize pulsed-laser pyrolysis successfully to obtain chemical information, one must carefully examine the physical processes which occur. After, and in fact during, the vibrational heating of the  $\text{SF}_6$  absorber by the  $\text{CO}_2$  laser radiation, vibrational-to-vibrational energy transfer occurs between  $\text{SF}_6$  molecules and the bath and sample molecules. After a sufficient number of these collisions, vibrational equilibration is attained. A degree of translational and rotational heating will accompany this process, since typical V-V transfer collisions are not resonant. It is possible, for some systems, that full thermalization will await the completion of slower V-T collisions. (It is even possible<sup>4</sup> for some gas mixtures, pressures, and degrees of

excitation to establish a steady-state non-equilibrium distribution of vibrational state populations.) To avoid these difficulties, it is preferable to choose a bath gas with a vibrational mode near the frequency of the absorbing  $\text{SF}_6$  mode ( $1000\text{ cm}^{-1}$ ), and with several other frequency modes suitably spaced. Ideally, some frequencies should be near-multiples of others, and the spacing of frequencies should roughly correspond to  $kT$  at some early point in the energy-transfer process ( $420\text{ cm}^{-1}$  at  $600\text{ K}$ ). On the other hand, the bath gas molecule cannot be so large that its heat capacity overwhelms the system with the result that only low temperatures can be reached. These conditions have led to our choice of small polyatomics, such as  $\text{SO}_2$ ,  $\text{NH}_3$ ,  $\text{CO}_2$ , or  $\text{CH}_4$ , as the bath gas.

It is difficult to estimate the time required for V-V equilibration, or for thermalization, since we are purposely dealing with higher temperatures and more complex mixtures than most previous studies of these processes.<sup>4</sup> At typical pressures of 100 torr, the gas kinetic collision frequency is roughly one per nanosecond. Since the pulsed-laser pyrolysis reaction time is roughly  $10\text{ }\mu\text{s}$ ,<sup>2e</sup> we require equilibration in approximately  $1\text{ }\mu\text{s}$  or 1000 collisions. Using a fast V-V rate for near-resonant processes of one per 100 collisions, this would require equilibration in ten energy transfer steps. However, since most V-V measurements have been made at lower temperatures and lower degrees of excitation, the rates pertinent to pulsed-laser pyrolysis could well be much faster. Some infrared fluorescence evidence to be presented later indicates sufficiently rapid equilibration does take place. The ultimate test, of course, lies in the ability to obtain relative decomposition yields for various substances in accord with their known kinetic parameters (see Section IV). The speed of energy transfer may place an upper limit on the useful temperatures attainable by this method.

Once rapid thermalization takes place, the gas cell contains a heated cylinder of gas (temperature  $T'$ ) surrounded by the cooler gas ( $T_0$ ), at the same density. Since the heated gas is now at a higher pressure, an acoustic compression wave now proceeds outward through the cool gas. The volume occupied by the heated gas expands, and the density and pressure fall, until the pressures on either side of the heated-gas-cold-gas interface are equal. This work is accomplished by a concurrent cooling (or rarefaction) wave propagating back to the center of the heated region. This cooling effectively quenches all but low activation energy reactions. If, however, the acoustic wave which continues outward through the cool gas (heating it very slightly) is allowed to reflect off the cell walls, it may return to reheat the heated region<sup>2e</sup> to reactive temperatures. We have utilized two strategies to avoid this complication. If the heated volume and the cell volume are not concentric, the reflected waves return at differing times, shapes, and strengths, and do not constructively reheat the sample.<sup>2e</sup> The experiments described later in this paper use a thin irradiated region surrounded by a wide torus-shaped volume which serves to dissipate the acoustic wave much like a shock-tube dump tank. A thin cell is used to insure that the sample is optically thin. Coupled with a rear mirror, this prevents non-uniform axial temperatures and longitudinal acoustic waves.

The remainder of this section discusses some infrared fluorescence experiments and some calculations pertaining to these acoustic wave phenomena and their implications for pulsed-laser pyrolysis experiments. While these waves are not, strictly speaking, shock waves, traveling below Mach 1, there are still some interesting contrasts and analogies with shock tube experiments. While both methods offer cold walls, similar cooling (or quenching) mechanisms, and similar comparative kinetics techniques, the shock tube heats by slower T-V transfer, has a somewhat longer reaction time, has a much lower duty cycle, typically

requires moderate vapor pressure substrates, and has a greater complexity. However, it can reach higher temperatures at present.

#### A. Experimental Diagnostics

By adding 5-10 torr of a strong IR fluorescer, such as  $\text{CH}_4$  or  $\text{CO}$ , to the gas mixture, one can monitor the time evolution of the temperature in the heated region by observing the emission intensity from  $V \geq 1$  at 3.3 or 4.6  $\mu\text{m}$ . The single-shot signal strength from a suitably filtered 1 MHz bandwidth InSb detector (Infrared Associates) is proportional to  $e^{-h\nu/kT}$ . Figure 3 illustrates the IR fluorescence from  $\text{CO}$  using  $\text{SO}_2$  bath gas and off-axis irradiation. We have previously reported some of these results.<sup>2e</sup> Some minor reheating effects of residual radial acoustic wave reflections are still evident. Rapid heating, within 3  $\mu\text{s}$ , is observed, although  $\text{CO}$  is not particularly fast for vibrational energy transfer. Cooling is observed in roughly 10  $\mu\text{s}$ . A peak temperature of  $\sim 1000$  K is estimated from measurements of absorbed laser energy and the known heat capacity data. The IR fluorescence then indicates cooling to 740 K. Further cooling then occurs by thermal conductivity and diffusion to the cool gas and eventually the cell walls, at an initial rate measured from the long-term decline of the IR signal of  $\sim 0.4$  K/ $\mu\text{s}$ . (A crude estimate from transport theory is 1.4 K/ $\mu\text{s}$ .) Under these conditions, for a reaction rate constant of  $\log k = 14.0 - 50.0/\theta$  ( $\theta = 2.303 RT$  in kcal/mole), 98% of the reaction occurs at 1000 K.

We have recently begun development of a new laser-based diagnostic for pulsed-laser pyrolysis which will furnish both temperature measurements and kinetic data.<sup>5</sup> Using laser-induced fluorescence of OH for two separate rotational lines of the A-X transition, both the temperature and relative OH densities can be measured. Pulsed-laser pyrolysis of  $\text{H}_2\text{O}_2$  is the OH source, and time-resolved data are obtained by varying the delay

between the  $\text{CO}_2$  laser and the pulsed UV dye probe laser. Equilibrium concentrations of OH appear to be maintained in the slowly cooling tail region of Figure 3. By adding  $\text{CH}_4$  and observing the decline of OH with time (10-200  $\mu\text{s}$ ), a bimolecular rate constant can be measured at elevated temperatures.

We are also investigating another alternate version of the pulsed-laser pyrolysis experiment. If the entire cell volume is irradiated, expansion of the heated region and the concurrent fast acoustic wave cooling are not possible. The gases will remain at hot, reactive temperatures for longer times, thus extending the experimental temperature range of the method to lower values without requiring an excessively large number of laser shots to accumulate reasonable yields. Figure 4 shows an infrared fluorescence trace under approximately these conditions. The reaction time near  $T_{\text{max}}$  has been extended to 30-50  $\mu\text{s}$ . Slow, gradual cooling is observed, although not as slow as the long-term cooling of Figure 3, since direct collisions with the walls remove energy more efficiently than the cool gas did. The advantage of cold unreactive walls remains. The cooling process, however, is not sudden, and temperature gradients will exist in the cell, thus making an analysis of kinetics more difficult for these experimental conditions. Comparative kinetics, spatially resolved diagnostics, and calculations should provide an indication of the usefulness of this version of the technique. Preliminary experiments on propyl chloride and ethyl acetate are consistent with the known parameters.

#### B. Calculations

To obtain a clear picture of the effects of these acoustic waves, we performed some calculations using the PUFF program at SRI. The simulated cell is filled with 100 torr  $\text{SO}_2$  and has a 7-cm diameter. It is divided into 14 concentric ring-shaped zones of .25-cm thickness.



(Zone 1 is a .25-cm radius cylinder.) The first three zones are "heated" from 300 K to temperature  $T_0$  in the first 1.0  $\mu$ s (heated area diameter, 1.5 cm). Each calculational zone's boundaries are allowed to expand or contract so the number of molecules it contains remains constant. The program then calculates the resulting gas dynamics without provisions for mass transport or thermal conductivity between the zones.

Figure 5 shows the time evolution of the temperatures in the heated zones 1-3 at various times after initial heating to 1000 K. Note the delay before the cooling wave reaches the innermost cell 1; that is, the longer reaction time. Cooling at any single spot is probably more rapid than shown, given the finite size of the cells used in the calculation. These results indicate the correct model for pulsed-laser pyrolysis is one whose reactive volume decreases with time. The average molecule remains hot for 8  $\mu$ s, and then cools to a generally nonreactive 800 K. The outgoing acoustic wave reflects and returns, however, at  $t = 240 \mu$ s and reheats the heated zone to temperatures slightly above 900 K for 25  $\mu$ s. For a 50 kcal activation energy reaction, this first reheating produces an extra 20% reaction, with later reflections adding diminishing yields. Since this alters the single kinetic temperature feature of the technique, such constructive reflections should be minimized.

This calculated behavior is in excellent agreement with the IR-fluorescence observations of Figure 3. Those results showed an initial cooling from  $\sim 1000$  K to 740 K completed within 20  $\mu$ s. When significant reheating is permitted by a concentric geometry,<sup>2e</sup> the times spent at the reheated temperature are longer than the initial reaction time, as evidenced by the greater widths of the subsequent IR peaks. The time scale for the reheating is much longer for the calculation than the experiment<sup>2e</sup> (240  $\mu$ s versus 60  $\mu$ s), because the cell diameter is larger (7 cm versus 3.8 cm). As the cylindrical compression wave moves outward, its area increases

and its velocity decreases--the extra 3.2 cm are traveled much more slowly. The calculated initial velocity of the wave is 150 m/s, roughly 65% of the speed of sound. This wave heats the initial portion of cool gas (cell 4) roughly 20 K.

As the compression wave moves outward, the volume occupied by the heated gas expands. The radius of the boundary between hot and cold gas (cells 3 and 4) is shown in Figure 6 as a function of time. It increases from 0.75 cm to 1.30 cm in the same time that the heated gas is cooling to 800 K. The expansion can be thought of as producing the cooling. The density and pressure also fall in this period. Figure 7 presents the density history of cells 1-3, for completeness. The inward-moving, cooling, expansion wave "reflects" off the singularity at the center of cell 1 and proceeds outward. This is responsible for the two-stage cooling observed for cell 3 in Figure 5. Note also that cell 1 appears to over-cool initially, likely due to the increased intensity of the wave as its area decreases on approaching the center. Once the cooling wave leaves cell 3 (outward-bound), all areas of the heated region remain in the same state, at least until any reflected waves return. At the boundary between cell 3 (hot) and cell 4 (cold), the pressures are equal at 90 torr. (Since the cells are still at vastly different temperatures, further cooling by thermal conductivity will occur across the boundary; a compressed region continues propagating through the cold gas.) When the reflected wave returns to reheat cells 1-3, the pressure will rise to 180 torr, and the heated zone radius will drop to 1.0 cm.

Similar behavior is seen for calculations with peak temperatures of 1200 K and 800 K. Table 1 summarizes some relevant results. The average reaction time for a molecule before cooling varies little. The proportional cooling in the expansion is virtually identical. Thus, temperature, as desired, is the only significant variable.

#### IV ERRORS RESULTING FROM TEMPERATURE VARIATIONS

Variations in temperature as a function of space and time can be substantial in the LPHP technique. For the cell geometry illustrated in Figure 1, where the laser beam is coincident with the axis of what is roughly a short cylindrical cell, the major variations will be as follows: First, if the laser beam has any Gaussian character whatsoever, the temperature will decrease as one moves radially outward from the cell axis to the full radius of the laser beam. Second, even if the peak temperature were uniform over the entire heated volume, the reaction time before the mixture is cooled by the rarefaction wave (which moves radially inward) will range from zero at the periphery of the heated zone up to the 10  $\mu$ sec transit time of the acoustic wave for reactants located at the cell axis. Third, unless reflected acoustic waves are damped, the cell contents in the originally heated region can be reheated to temperatures 100-200 K below the peak temperature, often repeatedly for total reaction times long relative to the initial 10  $\mu$ s period. Furthermore, even without this reheating, reaction might be possible after the acoustic wave cooling in the low temperature tail where slow thermal conductivity cooling occurs.

All of the above effects can be minimized by suitable tailoring of the reaction system and by measurement and deconvolution of the effects of these temperature and time variations. The former approach has been taken to some extent in the work presented here and is discussed in Section III. However, the discussion below shows that the errors caused by any (or all) of these effects can be readily limited by suitable choice of temperature standard and limitations in fractional decomposition. In

the worst cases, use of a second temperature standard having parameters which result in a bracketing of the unknown can eliminate any significant uncertainties concerning such errors.

#### A. Effects of Non-Isothermal Temperature-Time Distribution

Possible errors resulting from a change in temperature during the course of reaction were assessed with a model in which an isothermal "peak" temperature period is followed by an isothermal tail at  $\Delta T$  °C below the peak temperature (see Figure 8, inset). These conditions roughly model two possible non-isothermal situations: (1) reaction in the heated region after the initial acoustic wave cooling ( $\Delta T \sim 250$  K at 1200 K) before significant conductive cooling, modeled by a constant temperature,  $T - \Delta T$ , for  $9\tau_r$ , or (2) reaction during three successive reflected wave reheatings of duration  $3\tau_r$  ( $\Delta T \sim 100$  K). For each substrate at each peak temperature, the ratio of the apparent rate constant to the "true" rate constant is given by:

$$\frac{k_{\text{apparent}}}{k_{\text{true}}} = \frac{A \left[ e^{-E/RT} + b e^{-E/R(T-\Delta T)} \right]}{A e^{-E/RT}} = 1 + b \left[ e^{-\frac{E}{R} \left( \frac{\Delta T}{T(T-\Delta T)} \right)} \right] \quad (4)$$

where  $T$  is the peak temperature,  $\Delta T$  is the difference between peak and tail temperatures, and  $b$  is the ratio of the tail length to the time at the peak temperature. Since the  $A$ -factor has cancelled in equation (4) the relative error due to reaction in the tail depends only on the activation energy of the substrate in question. The solid line in Figure 8 shows the error resulting from an unknown which has an activation energy 11.5 kcal/mole higher than the standard ( $E_1 = 78.3$ ,  $E_2 = 66.76$ ) and conditions which provide: (1) an isothermal tail nine times longer than the peak temperature reaction time, and (2) a fixed  $\Delta T$  for all temperatures. The error goes through a maximum because when  $\Delta T$  is low there is no tail, and when  $\Delta T$  is high, there is no reaction in the tail.

In the case modeled, the maximum error from this non-isothermal distribution is  $\sim 2$  kcal/mole at  $\Delta T = 160^\circ\text{C}$ . A physically more realistic picture is one in which the fractional decrease in temperature is constant (see calculations of Section III). Thus, when  $\Delta T = 160^\circ$  at 1400 K,  $\Delta T$  will be  $\sim 148^\circ$  at 1300 K, and the dashed line in Figure 8 indicates that for these values, the error will be less than half the 2 kcal/mole expected for equal  $\Delta T$  values of  $160^\circ\text{C}$ . Furthermore, the single point in Figure 3 indicates that with the expected proportional values of  $\Delta T$  and a closer match between the standard and unknown activation energies ( $E_2 - E_1 = -5$  kcal/mole), the error in  $E_1$  would actually be only  $\sim -0.3$  kcal/mole. The errors in the Arrhenius A-factor correspond roughly to those in the activation energy; that is,  $\Delta \log A \approx \frac{\Delta E}{4.576 T}$ . Thus, a derived activation energy which is too low by 0.3 kcal/mole would be accompanied by a derived A-factor that is too low by  $\sim 0.05$  log units.

#### B. Effects of Non-Isothermal Temperature-Space Distribution

The effects of variations in temperature with space were assessed by modeling the system as two equal coaxial reaction volumes, an inner cylinder, and a lower temperature annular space (see inset, Figure 9). For each substrate, the ratio of the apparent rate constant to the true rate constant is determined by measuring the averaged contents of the reaction cell and is given by:

$$\frac{k_{\text{apparent}}}{k_{\text{true}, T_2}} = \frac{\ln 2 - \ln \left[ e^{-(A_1 e^{-E/RT_1}) \tau_r} + e^{-(A_1 e^{-E/RT_2}) \tau_r} \right]}{(A_1 e^{-E_1/RT_2}) \tau_r} \quad (5)$$

where  $T_1$  and  $T_2$  are the lower and higher temperature regions. In contrast to equation (4), which describes the ratio of the apparent to the true rate constant for reaction in a temperature-time tail, there is no cancellation of the A-factor. In equation (5), it is the absolute rates at the two temperatures rather than the activation energy that determines the

error in rate constant. This is illustrated by Figure 4 in which the error in the derived activation energy is plotted as a function of the temperature difference  $\Delta T$  between the high and low temperature regions. All four plots are for the same two activation energies: the only difference is in the A-factors and hence in the absolute rates and observed fractional decompositions. Plot (a) indicates that: (1) if the fractional decomposition (per shot) is limited to  $\leq \sim 30\%$ , the error in E will be  $\leq \sim 1$  kcal, and (2) if the fractional decomposition of the standard (compound 2) is less than that of the unknown, the temperature dependence of the unknown will be under-represented, and the value of  $E_1$  determined will be too low. Plots (c) and (d) illustrate that if the fractional decomposition of the standard is greater than that of the unknown, the temperature dependence of the unknown will be exaggerated and the value of  $E_1$  determined will be too high. This holds irrespective of whether the standard or the unknown has the higher activation energy. As in the case of temperature-time variations, an activation energy that is too low will be accompanied by an A-factor that is too low.

C. Effect of Variation in Reaction Time with Substrate Location in the Reaction Cell

The effect of using an average reaction time in a situation where the actual reaction times range from zero to  $10 \mu\text{sec}$  is similar to the effect of the temperature-space variations discussed above. The errors depend on the absolute rates of the substrate and the standard and not upon their activation energies per se. The cases modeled in section IV-B suggest this error will be small as long as the fractional decomposition is held below  $\sim 25\%$  (per shot, at the higher temperature, averaged over the entire reaction volume). Similarly, an analytical treatment of this source of error indicates it can be readily held to a minimum.

The analysis of Reference 2e, assuming as the simplest case a heated volume linearly decreasing with time, gave  $Y = \frac{A\tau_0}{2} e^{-E/RT} - \frac{A^2\tau_0^2}{6} e^{-2E/RT} \dots$  where Y is the single-shot fractional decomposition within the heated region, and  $\tau_0$  is the time required to cool the entire heated volume ( $\tau_0 = 2\tau_R$ ). On the other hand, assuming the entire volume remains heated for time  $\tau_0/2$  gives:

$$-\ln(1-Y) = \frac{A\tau_0}{2} e^{-E/RT} = k(\tau_0/2)$$

or

$$1 - Y = e^{-k\tau_0/2}$$

A power series expansion shows:

$$Y = \frac{A\tau_0}{2} e^{-E/RT} - \frac{A^2\tau_0^2}{8} e^{-2E/RT} \dots$$

Except in the limit of high yields (>10%), only the identical first terms are important. The 25% difference in the second term is significant only at very high fractional decompositions where reliable application of the technique is likely to be difficult. For a 50 kcal/mole activation energy reaction, at a yield of  $Y = 0.18$ , the difference is only 4%. The error introduced in a derived  $E_a$  by using the imprecise analysis would be less than 0.6 kcal/mole.

## V RESULTS AND DISCUSSION

### A. Molecular Elimination Reactions

The absence of secondary reactions as a complicating factor generally makes molecular eliminations the first choice for demonstrating the capabilities of any technique used to determine Arrhenius parameters. Thus our initial experiments were done using substrates of this type whose Arrhenius parameters are well known.<sup>6</sup>

A mixture of ethyl acetate, isopropyl acetate, isobutyl bromide,<sup>6</sup> SF<sub>6</sub> and CO<sub>2</sub> was passed through the LPHP flow system shown in Figure 1 and allowed to decompose at a range of laser intensities. The temperatures in the laser heated region ranged between 950 K to 1100 K and produced fractional decompositions up to 45% per shot. Figure 10 shows the resulting data, plotted as  $\log k_1 \tau_r$  versus  $\log k_2 \tau_r$ . The solid lines represent the relationships expected from the values of the Arrhenius parameters reported in the literature. The correspondence between these three lines and the data illustrates that using any one of the three as a comparative rate "standard" to determine the parameters of either of the other two as an "unknown" reproduces the literature parameters to within a few percent.

This consistency in an over-determined system strongly suggests that the agreement of any pair with the reported Arrhenius parameters is not fortuitous. Therefore, we conclude that (1) temperature accommodation for the three substrates is effectively identical and (2) the temperature-time-space variations discussed above in fact do not introduce significant systematic error.

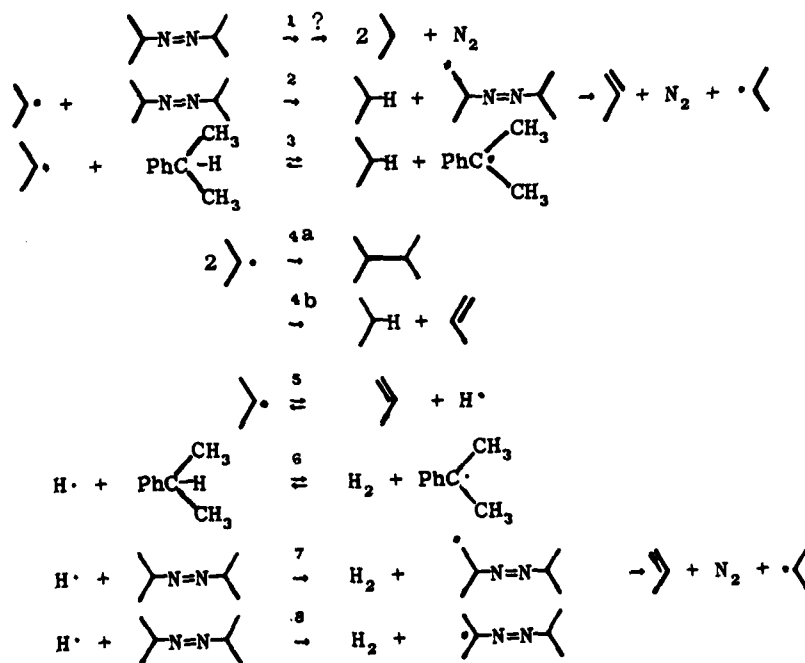
Consideration of the observed errors reveals no correlation with either the difference in rates or the difference in activation energies of the "unknown" and standard. Thus, it is clear that systematic errors are relatively unimportant under these conditions and Arrhenius parameters can be determined with acceptable accuracy even when the range of rate data is only modest and the fractional decomposition ranges up to 45%. The data in Figure 5, which cover somewhat less than two orders of magnitude in rate, were obtained with a Hewlett-Packard 5750 gas chromatograph. The HP 5711 chromatograph currently being used has a higher usable sensitivity and will allow this range to be significantly extended and the precision correspondingly increased.



## B. Radical-forming Reactions

Since the intended application of LPHP in our laboratories is to wall-sensitive radical-forming reactions, it was also necessary to demonstrate that the technique is practical in cases where radicals or other reactive products are formed. Such products can readily bring about chain decomposition and other complicating secondary reactions that can drastically distort the decomposition rate temperature dependence. For such a demonstration, we chose azoisopropane, since its decomposition produces simple radical products in the temperature range of the alkyl acetate molecular elimination processes we had already surveyed.<sup>7</sup> The decomposition of dialkyl azo-compounds has been recently discussed in a thorough review by Engel,<sup>7</sup> where the accepted parameters for azoisopropane (AIP) are given as  $\log k \text{ (sec}^{-1}\text{)} = 16.6 - 47.9/2.303 \text{ RT}$ .

Under LPHP conditions, the reactions of azoisopropane that must be considered are:



Consideration of reported data on H-abstraction reactions<sup>8</sup> indicates that, in the temperature range 800 to 1000 K, neither reaction (3) nor reaction (4) should be competitive with reaction (5).<sup>9</sup> The use of a scavenger to remove H-atoms is thus necessary and conditions must be arranged to ensure that reaction (6) greatly exceeds reaction (7).

The LPHP technique was used, with an excess of either toluene or cumene as a scavenger and t-butyl acetate as a temperature standard, to measure the temperature dependence of azoisopropane decomposition. The data are shown in comparative rate form in Figure 11. These data clearly show that azoisopropane decomposition under these conditions exhibits a temperature dependence and absolute reaction rates that are far too low to be compatible with the behavior anticipated on the basis of the accepted parameters,  $\log k = 16.6 - 47.9/2.303 RT$ . However, the present data are in good agreement with the data of Ramsperger<sup>10</sup> and of Geiseler and Hoffman.<sup>11</sup> In Figure 12, all reported data for gas-phase trans-azoisopropane decomposition<sup>10-12</sup> are represented. The internal temperature dependence of LPHP data is the same as the low temperature data of Ramsperger and of Geiseler and Hoffman, i.e., each set extrapolates very well to the other, covering a total temperature range of 500°C. Of greater significance, however, is the fact that the LPHP absolute rates are an order of magnitude too low to be consistent with parameters of  $10^{16.6} \text{ sec}^{-1}$  and 47.9 kcal/mole. Measured absolute rates that are too low by an order of magnitude could reasonably be explained under our conditions only by secondary reactions which consume ~ 90% of the initial products. This possibility is highly unlikely, since the data shown in Figure 11 include a change in scavenger from toluene to cumene and an increase in the amount of scavenger to a thousand-fold excess over azoisopropane. At this level of scavenger, secondary products (including di-isopropyl) were not detectable ( $\leq 0.2\%$  of propylene).

Furthermore, although small flow variations and low fractional decomposition typically make an exact mass balance difficult to establish, the total products never leave more than 15% of the decomposed starting material unaccounted for.

In addition, rates that are low by an order of magnitude cannot be the result of AIP decomposition being in the falloff. RRK estimates indicate that even if the correct Arrhenius parameters were  $\log k = 16.6 - 47/2.3 \text{ RT}$ , AIP decomposition under LPHP conditions at the upper end of the temperature range utilized ( $\sim 1000 \text{ K}$ ) would be in the falloff by less than 20% (i.e.,  $k/k_{\infty} \approx .82$ ). For any set of parameters with a lower A-factor, the decomposition will be less in the falloff, such that for  $\log k = 13.9 - 40.7/2.3 \text{ RT}$ ,  $k/k_{\infty} \geq 0.96$ . Over the range 900 to 1000 K the maximum tilting of an Arrhenius plot that would result from falloff associated with these lower parameters would be 0.6%, and would result in an apparent lowering of the temperature dependence by an almost insignificant 0.2 kcal/mole.

Thus, the LPHP data make the conclusion all but inescapable that the thermal decomposition of azoisopropane is correctly described by Arrhenius parameters in the range of  $10^{13.75} \text{ sec}^{-1}$  and 40.9 kcal/mole. The unequivocal nature of these LPHP data notwithstanding, similar measurements in another radical-forming reaction in which the "well known" Arrhenius parameters are reproduced are desirable. Such measurements are planned using t-butyl nitrite as a substrate.

Since an A-factor of  $\leq 10^{14} \text{ sec}^{-1}$  at 900 K means that  $\Delta S^{\ddagger} \leq 1.3 \text{ e.u.}$ , we conclude as well that the mechanism of decomposition, at least for azoisopropane, does not involve the scission of only one bond, but probably involves the more extensive reorganization associated with simultaneous loss of both alkyl groups. Simultaneous cleavage of two bonds would not

appear to be supported by the high A-factors that have been reported<sup>12a,b,13</sup> for 2,2-azoisobutane ( $\log A_{\text{avg}} = 16.56 \pm 0.71$ ; one  $\sigma$ , six studies). The decomposition of this azoalkane (AIB) is least subject to secondary reactions and has provided various investigators with the most consistent sets of Arrhenius parameters. However, simultaneous cleavage is entirely consistent with other studies of azoalkane decomposition in which first one and then the other alkyl group is made more hindered and/or capable of producing a more stable alkyl radical.<sup>14</sup> The implications of these studies have sometimes been obscured by attempts to use differences in experimental activation energies as the indicator of the effects of substitution, but as Engel points out,<sup>7</sup> simple comparison of relative rates ( $\Delta\Delta G^{\ddagger}$ ) makes it very difficult to avoid the conclusion that the rate is increased by changes that increase the relative stability of not just one, but of both the incipient radicals. Thus, the effect of sequential alkyl substitution suggests that both radicals must be partially (though not necessarily equally) formed in the transition state.

A re-examination of the kinetic studies of AIP and AIB decomposition in which high A-factors have been reported<sup>13</sup> did not, in most cases, reveal any compelling basis for rejecting the stated parameters. However, cases where unanticipated systematic errors make the actual errors in Arrhenius parameter measurements far exceed the random errors are as much the rule as the exception. Therefore, in our judgement, the most probable parameters for AIP decomposition are given by a line drawn through the low temperature data and the high temperature LPHP data at the mid-point of their respective temperature ranges. This results in  $10^{13.9} \text{ sec}^{-1}$  and 41.2 kcal/mole, essentially indistinguishable from the  $10^{13.6} \text{ sec}^{-1}$  and 40.0 kcal/mole provided by the LPHP data themselves.

Having concluded that the present data in all probability rule out the alternative high Arrhenius parameters, it is nevertheless informative to consider the implications of the opposite conclusion. If the operative

mechanism for AIP decomposition were sequential bond scission, then the activation energy (48 kcal/mole) corresponding to a high A-factor (i.e., to  $10^{18.6} \text{ sec}^{-1}$ ) would be correct and would roughly equal the bond dissociation energy in  $\text{iPrN=N-iPr}$ . By comparison with the analogous C-C bond in  $\text{iPrCH=CH-iPr}$  at 95 kcal/mole, this bond is 47 kcal/mole weaker than what one would expect for a bond between an i-propyl group and a "normal"  $\text{sp}^2$  center. By this operational definition, the  $\text{RN=N}\cdot$  radical exhibits a very large resonance stabilization energy. The question is, is this reasonable, given that the contributing structure pictured as being responsible for the stabilization ( $\text{RN=N}$ ) has one electron in an anti-bonding orbital. The considerations below suggest at least that it is not unreasonable and therefore that a 48 kcal/mole bond strength could not have been ruled out on an a priori basis.

Let us consider bond strengths in the series  $\text{H}_2\text{C=CH-H}$ ,  $\text{H-CHO}$ , and  $\text{HN=N-H}$  as being related to what we will call "pseudo"  $\pi$ -bond strengths in acetylene, carbon monoxide, and nitrogen. The pseudo- $\pi$ -bond strengths are defined as the energy released by formation of the triple bond from the canonical, non-interacting forms,  $\text{HC}\equiv\text{CH}$ ,  $\text{C}\equiv\text{O}$ , and  $\text{:N}\equiv\text{N:}$ . The heats of formation of these hypothetical structures are derived by assuming that scission of all bonds  $\text{X-H}$ , where X is an  $\text{sp}^2$  hybridized carbon, nitrogen, or oxygen, costs 110 kcal/mole if interaction with unpaired or unshared pairs of electrons on adjacent atoms is precluded. This assumption is realized, of course, only for the first C-H bond in ethylene, from which the value 110 kcal/mole is derived.<sup>15</sup> This definition, together with measured heats of formation for the triply bonded species and their hydrogenated forms,<sup>16,17</sup> results in pseudo- $\pi$ -bond strengths for  $\text{HC}\equiv\text{CH}$ ,  $\text{C}\equiv\text{O}$ , and  $\text{N}\equiv\text{N}$  of 74, 116, and 166 kcal/mole, respectively. Linear extrapolation of the assumed correlation between measured  $\text{H}_2\text{C=CH-H}$  and  $\text{H-CHO}$  bond strengths and pseudo- $\pi$ -bond energy leads to an estimated  $\text{HN}_2\text{-H}$  bond strength in diimide of 62 kcal/mole. Since the  $\text{iPrCH=CH-iPr}$  bond is known<sup>18</sup>

to be 15 kcal/mole weaker than the  $i\text{PrCH}=\text{C}-\text{H}$  bond, a reasonable expectation for  $i\text{PrN}=\text{N}-i\text{Pr}$  would then be  $62 - 15 = 47$  kcal/mole, exactly what a sequential-bond-scission interpretation of the low temperature AIP decomposition data would suggest. This is in good agreement with the bond strength derived from appearance potential measurements<sup>17</sup> and theoretical calculations<sup>18</sup> of the heat of  $\text{HN}_2\cdot$  decomposition. Since these estimations and calculations could easily be in error by  $\pm 15$  kcal/mole, existing thermochemical data would not allow us to state a priori that a 47 kcal/mole resonance stabilization energy is unrealistic for the  $\text{RN}=\text{N}\cdot$  radical. Thus, existing data would suggest a one-bond scission pathway may not be much less favored for AIP than the simultaneous bond scission pathway that the present LPHP data indicate is operative for AIP.

On the other hand, known thermochemical data also indicate that synchronous bond cleavage might have been expected. Recent measurements of the heat of formation of trans-azoisopropane<sup>7</sup> reveal that the overall reaction



is endothermic by 26 kcal/mole. This is 2 kcal/mole less than a sequential bond scission interpretation of AIP decomposition data would indicate for the  $i\text{PrN}=\text{N}-i\text{Pr}$  bond strength. The decomposition of the intermediate radical  $i\text{PrN}=\text{N}\cdot$  would then have to be 22 kcal/mole exothermic. While this exothermicity does not make sequential decomposition unreasonable, it does illustrate the substantial driving force that exists for formation of the  $\text{N}=\text{N}$  bond. It also suggests that synchronous cleavage of the two N-alkyl bonds could result in a pathway that benefits from the strength of the second  $\pi$ -bond and circumvents the need to go all the way over an extra 22 kcal/mole "hill".

These considerations, in combination with the LPHP results, are consistent with Engel's generalization<sup>7</sup> that symmetrical azo compounds appear to decompose by way of a synchronous bond scission pathway, but that little asymmetry is required (in terms of differing R<sup>•</sup> and R<sup>•</sup>' stability) before the one-bond scission pathway is favored. Current efforts<sup>19</sup> to provide improved, ab-initio calculations of bond strengths in di-imide structures, as well as planned LPHP studies of azoisobutane decomposition, may help to further clarify the azo compound decomposition picture.

#### ACKNOWLEDEMENTS

The authors wish to acknowledge the support of the Army Research Office, Contract No. DAAG29-78-C-0026, and the National Science Foundation, Grant No. CHE79-23569, and to thank Dr. Lynn Seaman for performing the acoustic wave calculations.

# REFERENCES AND NOTES

1. See, for example:
  - (a) Schulz, P. A.; Sudbo, Aa. S.; Krajnovich, D. J.; Kwok, H. S.; Shen, Y. R.; Lee, Y. T. Ann. Rev. Phys. Chem. 1979, 30, 379.
  - (b) Letokhov, V. S.; Moore, C. B. in Chemical and Biochemical Applications of Lasers, C. B. Moore, ed., 1977, 3, 1, Academic Press: New York.
  - (c) Golden, D. M.; Rossi, M. J.; Baldwin, A. C.; Barker, J. R. Accounts of Chemical Research 1981, 14, 56.
2.
  - (a) Shaub, W. M.; Bauer, S. H. Int. J. Chem. Kinetics, 1975, 7, 509; Shaub, W. M., Ph.D. Thesis, Cornell University 1975.
  - (b) Steel, C.; Starov, V.; Leo, R.; John, P.; Harrison, R. G. Chem Phys. Lett. 1979, 62, 121.
  - (c) Zitter, R. N.; Koster, D. F.; Cantoni, A.; Pleil, J. Chemical Physics, 1980, 46, 107.
  - (d) Lewis, K. E.; McMillen, D. F.; Golden, D. M. J. Phys. Chem. 1980, 84, 227.
  - (e) Smith, G. P.; Laine, R. M. J. Phys. Chem. 1981, 85, 1620.
  - (f) Berman, M. R.; Comita, P. B.; Moore, C. O.; Bergman, R. G. J. Am. Chem. Soc. 1980, 102, 5692.
3.
  - (a) Tsang, W. J. Chem. Phys. 1964, 40, 1171.
  - (b) Tsang, W. J. Chem. Phys. 1964, 41, 2487.
  - (c) Tsang, W. J. Phys. Chem. 1972, 76, 143.
4. Baily, R. T.; Cruickshank, F. P., Specialist Periodical Report, Gas Kinetics and Energy Transfer, The Chemical Society: London, 1978; p. 109.
5. Crosley, D. C.; Smith, G. P., preliminary results.
6. Benson, S. W.; O'Neal, H. E. Kinetic Data on Gas-Phase Unimolecular Reactions: National Standard Reference Data System, NSRDS-NBS 21, 1970; pp. 158, 169, 94, 189.
7. Engel, P. S. Chem. Rev. 1980, 80, 99
8. Kerr, J. A.; Parsonage, M. J. Evaluated Kinetic Data on Gas-Phase Hydrogen-Transfer Reactions of Methyl Radicals; Butterworths: London, 1976.



9. Reference 6, p. 572.
10. Ramsperger, H. C. J. Am. Chem. Soc. 1928, 50, 714.
11. Geiseler, G.; Hoffman, J. Z. Physik. Chem. 1968, 57, 318.
12. (a) McKay, G.; Turner, J.M.C.; Zare, F. J. J. Chem. Soc., Trans. Faraday Soc. I, 1977, 72, 803.  
(b) Martin, G.; Maccoll, A. J. Chem. Soc., Perkin Trans. 2, 1977, 1887.  
(c) Acs, G.; Peter, A.; Huhn, P. Int. J. Chem. Kinetics 1980, 12, 993.  
(d) Perona, M. J.; Beadle, P. C.; Golden, D. M. Int. J. Chem. Kinetics 1973, 5, 495.
13. (a) Blackham, A. V.; Eatough, N. L. J. Am. Chem. Soc. 1962, 84, 2922.  
(b) Levy, J. B.; Copeland, B.K.W. J. Am. Chem. Soc. 1960, 82, 5314.
14. Garner, A. W.; Timberlake, J. W.; Engel, P. S.; McLaugh, R. A. J. Am. Chem. Soc. 1975, 97, 7377.
15. Kerr, J. A.; Trotman-Dickenson, A. F. in Handbook of Chemistry and Physics, 57th ed.; Chemical Rubber Co.: Cleveland, Ohio, 1976; p. F-231.
16. Benson, S. W. Thermochemical Kinetics, 2nd ed.; John Wiley and Sons: New York, 1976.
17. Foner, S. N.; Hudson, R. L. J. Chem. Phys. 1978, 68, 3162.
18. Baird, N. C. J. Chem. Phys. 1975, 62, 380.
19. Goddard, W. private communication.

## Appendix

### DERIVATION OF THE EXPRESSION FOR THE REACTION RATE CONSTANT AS A FUNCTION OF THE OBSERVED STEADY-STATE FRACTIONAL DECOMPOSITION

If  $A_{ss}$  is the concentration of the substrate at "steady state" just before any individual laser shot (i.e., the top of the sawtooth pattern in Figure 2), then the decrease in average concentration during any single laser shot (at steady state) is given by:

$$A_{ss} \frac{V_R}{V_T} \left( 1 - e^{-k\tau_r} \right) \quad (A-1)$$

where  $\tau_r$  is the reaction time following each laser pulse, and  $V_T$  and  $V_R$  are the total and laser-heated volumes, respectively. The total (accumulated) decrease from  $A_0$ , the laser-off steady-state concentration, to the concentration established immediately following any single "steady-state" laser pulse is given by:

$$(A)_0 - A_{ss} \left[ 1 - \frac{V_R}{V_T} \left( 1 - e^{-k\tau_r} \right) \right] \quad (A-2)$$

The replenishment, by flow, which takes place before the next laser shot is then given by the total net loss multiplied by a term describing the fractional replenishment:

$$\left[ A_0 - A_{ss} \left[ 1 - \frac{V_R}{V_T} \left( 1 - e^{-k\tau_r} \right) \right] \right] \left( 1 - e^{-\tau_l/\tau_F} \right) \quad (A-3)$$

where  $\tau_l$  is the time between laser pulses (typically 4 sec), and  $\tau_F$  is the flow lifetime in the reaction cell (typically 200 sec). At "steady state" the decrease following any single laser shot equals the replenishment before the next shot. This results in equation (A-4):

$$A_{ss} \left(1 - e^{-k\tau_r}\right) \frac{V_R}{V_T} = \left[ (A)_o - A_{ss} \left[ 1 - \frac{V_R}{V_T} \left(1 - e^{-k\tau_r}\right) \right] \right] \left(1 - e^{-\tau_l/\tau_F}\right)$$

Rearranging and taking the logarithm of both sides results in equation (A-5):

$$k\tau_r = -\ln \left[ 1 - \left( \frac{A_o}{A_{ss}} - 1 \right) \frac{V_T}{V_R} \left( \frac{1 - e^{-\tau_l/\tau_F}}{e^{-\tau_l/\tau_F}} \right) \right] \quad (A-5)$$

Under typical conditions, when the values of  $\tau_r$ ,  $\tau_l$ , and  $\tau_F$  are 10  $\mu$ sec, 4 sec, and 200 sec, respectively, equation (A-4) is satisfactorily approximated by:

$$k\tau_r \approx -\ln \left[ 1 - \left( \frac{A_o}{A_{ss}} - 1 \right) \frac{V_T}{V_R} \left( \frac{\tau_l}{\tau_F} \right) \right] \quad (A-6)$$

Although equations (A-5) and (A-6) result from the definition of  $A_{ss}$  as the concentration just before any individual laser shot, gc analysis actually provides a value somewhere in between the top and the bottom of the pattern. Under the conditions stipulated above, the maximum error which could result from this sampling time uncertainty would be  $\sim 4\%$ , and the average error would be only  $\sim 2\%$ . This would, in any case, be a random and not a systematic error.

Table 1  
ACOUSTIC WAVE CALCULATIONS

$T_{\text{max}}$ (K)	800	1000	1200
$T_{\text{cool}}$ (K)	660	800	940
$t_{\text{hot}}$ ( $\mu\text{s}$ )			
cell 1	16	14	14
cell 2	12	10	9.5
cell 3	5	5	4
AVG ( $\tau_R$ )	8.6	7.7	6.8

# FIGURE CAPTIONS

- 1 Schematic of Laser-Powered Homogeneous Pyrolysis Flow System
- 2 Schematic Representation of the Spatially Averaged Substrate Concentration as a Function of Time.
- 3 Time Evolution of CO Infrared Fluorescence for Off-Axis LPHP Irradiation.
- 4 Time Evolution of CO Infrared Fluorescence for Irradiation of Entire Cell Volume.
- 5 Calculated Temporal Temperature Distributions for Three Concentric LPHP-Irradiated Regions. Cell 3 is the outermost 0.25-cm wide ring.
- 6 Calculated Boundary Radius of the LPHP-heated Region Versus Time.
- 7 Calculated Temporal Density Distributions for Conditions of Figure 5.
- 8 Calculated Effect of Temperature-Time Tail on Error in Derived Activation Energy. The calculation is for an unknown and a standard that have actual activation energies  $E_1$  and  $E_2$  of 78.3 and 66.76 kcal/mole, respectively. It is based on equation (4) which applies to the simplified situation shown in the figure inset: isothermal tails which are  $\Delta T_1$  and  $\Delta T_2$ , °C, respectively, below the peak temperatures  $T_1$  and  $T_2$  at the low and high temperature extremes of the Arrhenius plot (1300 and 1400 K).  
  

—  $\Delta T_1$  and  $\Delta T_2$  equal and variable, as indicated.

----  $\Delta T_2$  equals 160°C,  $\Delta T$ , as indicated

$\Delta T_1 = (T_1/T_2)\Delta T_2$ ,  $\Delta T_2 = 160^\circ\text{C}$ .
- 9 Calculated Effect of Non-Isothermal Temperature-Space Distribution on Error in Derived Activation Energy. The calculation is for an unknown and a standard that have actual activation energies of 60 and 65 kcal/mole, respectively. It is based on application of equation (5) to the simplified situation shown in the figure inset, a cylindrical inner, hotter volume, and an annular space  $\Delta T$  °C

cooler. Activation energy is determined by a two-point plot over the nominal temperature range 800 to 900 K. For the plots a,b,c, and d, the fractional decomposition at 900 K per shot, in the heated region, for Compound 1 (unknown) and Compound 2 (standard) respectively, are:

(a) 48% and 28%; (b) 72% and 48%, (c) 7% and 48%, and (d) 7% and 15%.

10 Simultaneously Determined LPHP Comparative Rate Plots for Molecular Elimination Reactions.

- Δ i-butylbromide versus i-propyl acetate
- i-butylbromide versus ethyl acetate
- i-propyl acetate versus ethyl acetate

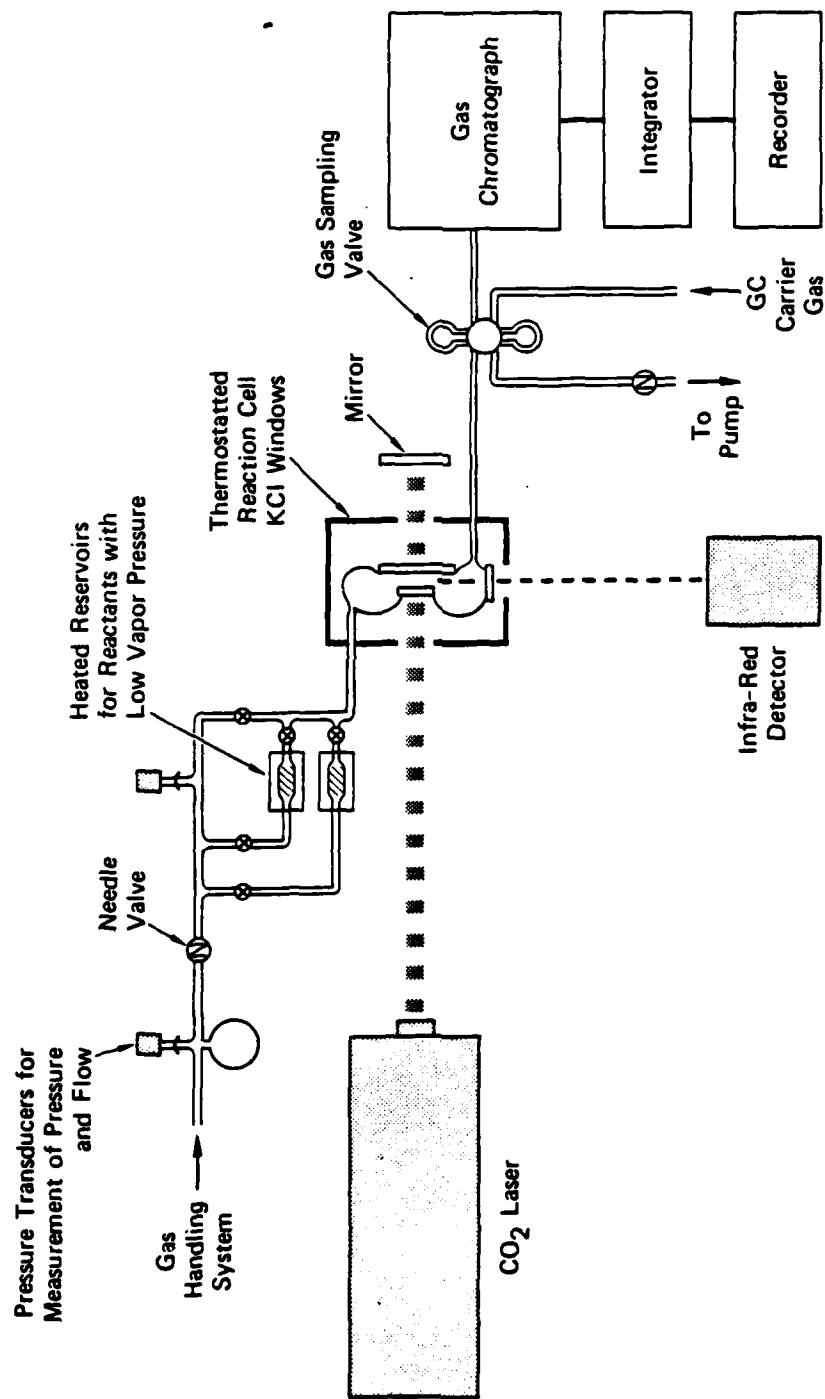
11 LPHP Comparative Rate Data for Azoisopropane and t-Butyl Acetate Decomposition

-----  $\log k_{AIP} = 16.45 - 47.5/2.303 RT$   
 -----  $\log k_{AIP} = 13.0 \pm .5 - 37.9 \pm 1.6/2.303 RT$   
 -----  $\log k_{AIP} = 13.6 - 40.0/2.303 RT$

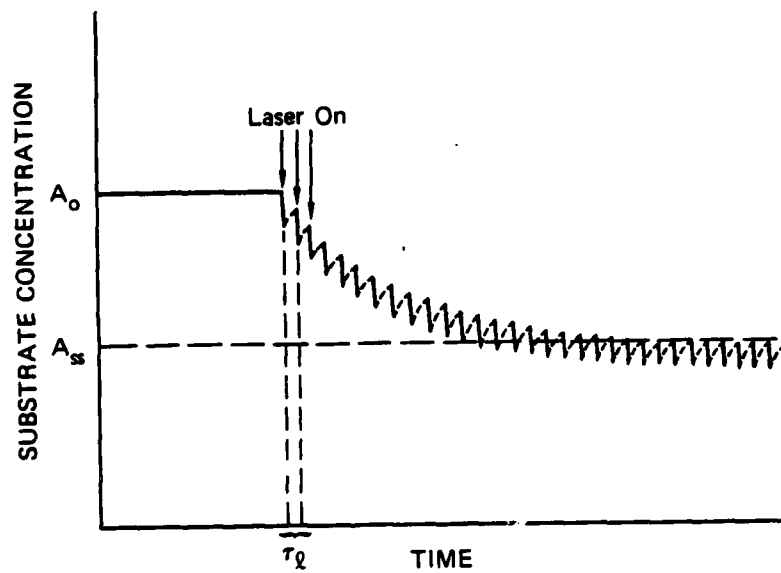
12 Azoisopropane Decomposition Rate as a Function of Temperature-- Collected Data.

Points representing literature results are not individual data points but represent values at the temperature extremes of the respective Arrhenius plots.

- □ Ramsperger, Reference 10,  $\log k = 13.75 - 40.9/2.303 RT$
- △ Geiseler and Hoffman, Reference 11.
- ▽ Geiseler and Hoffman, Reference 11.
- ◇ Acs et al., Reference 12(c).
- McKay et al., Reference 12(a).
- Perona et al., Reference 12(d). Lines do not represent raw data, but VLPP data fitted via RRKM falloff estimates, to either  $\log k = 16.6 - 47.9/2.303 RT$ , or  $\log k = 13.75 - 40.9/2.303 RT$
- -- LPHP data; this work,  $\log k = 13.6 - 40.0/2.303 RT$

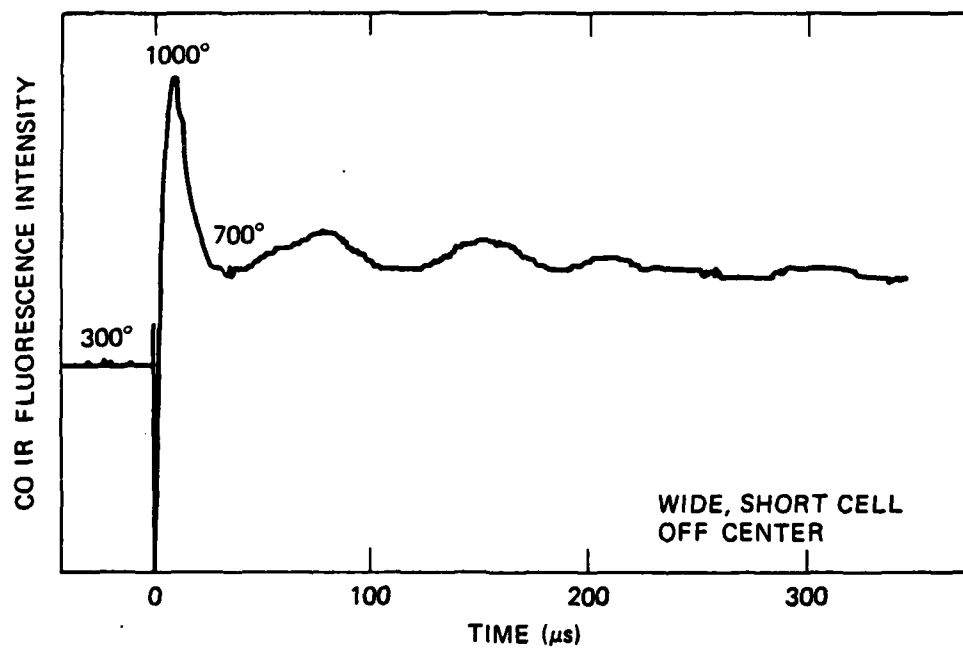


JA-322522-5

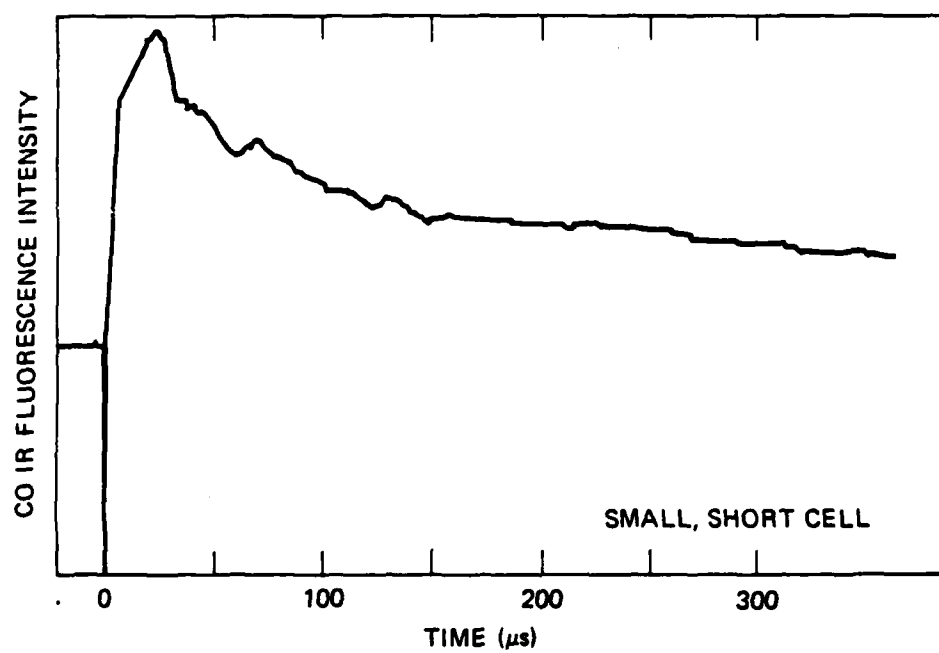


JA-322522-6

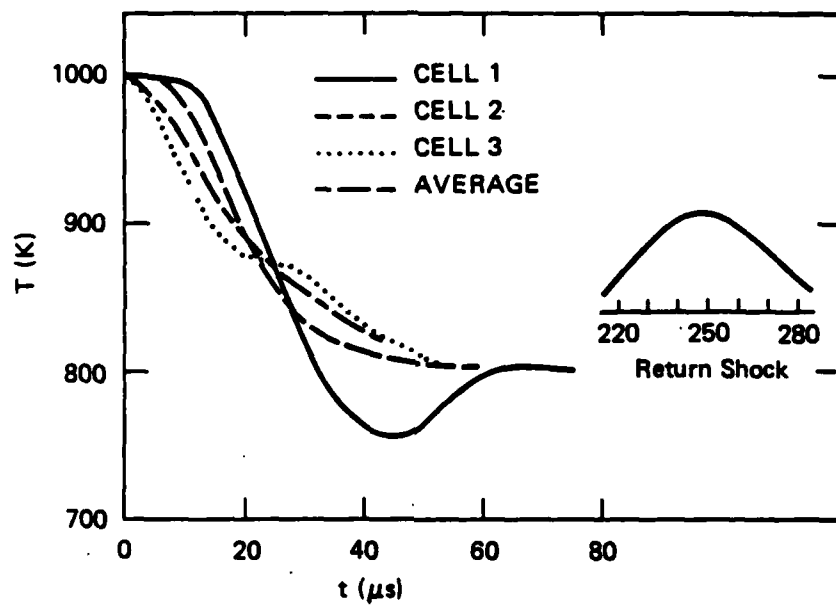




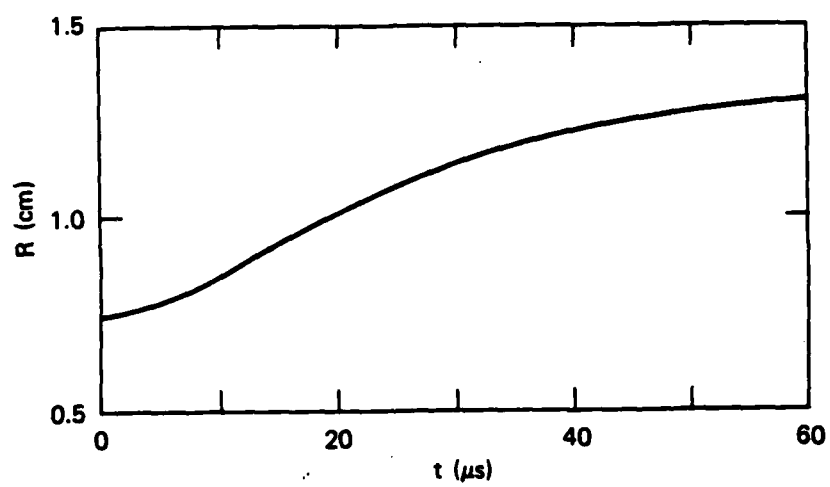
JA-322543-1



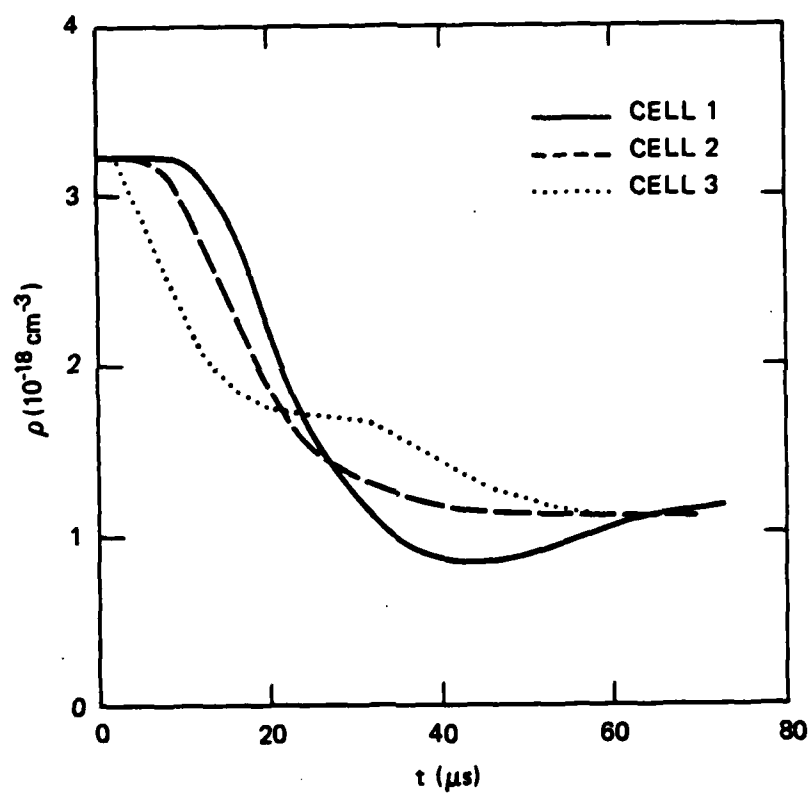
JA-322543-2



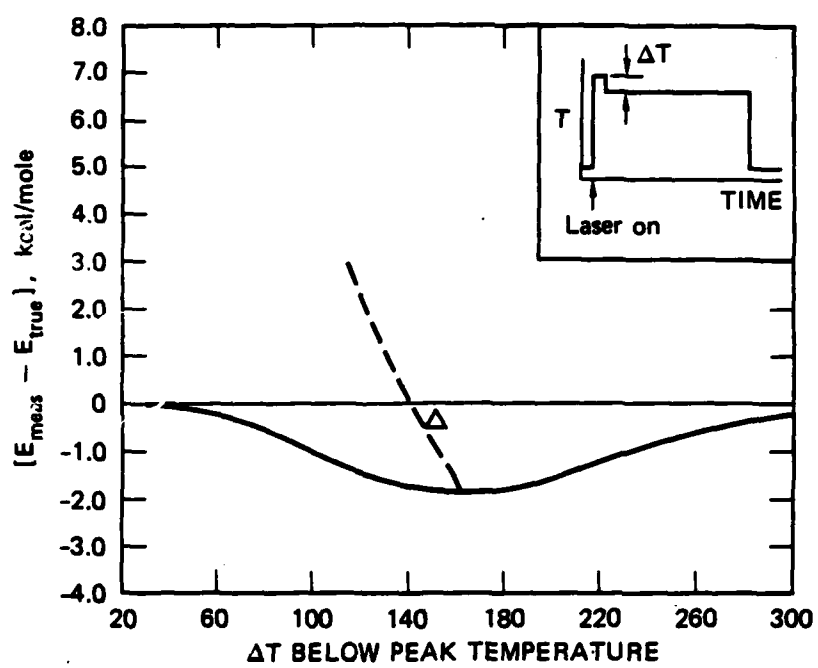
JA-2088-3



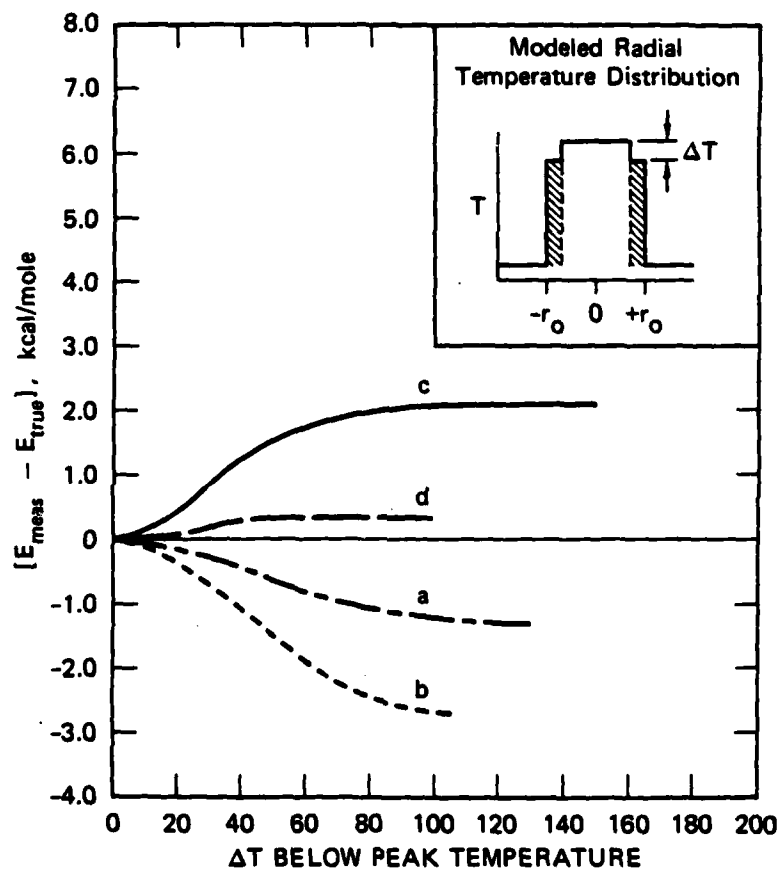
JA-2066-4



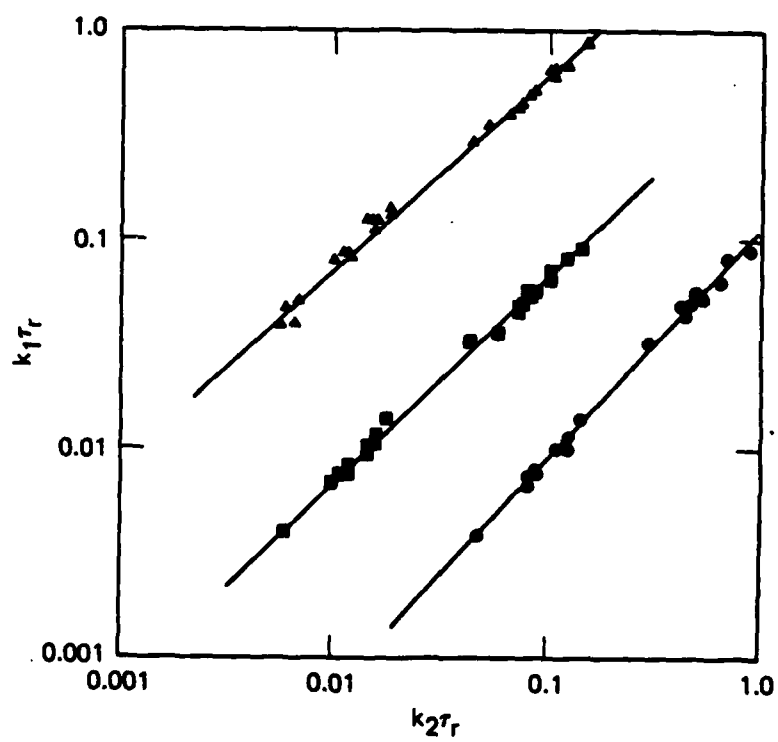
JA-2086-2



JA-322522-7

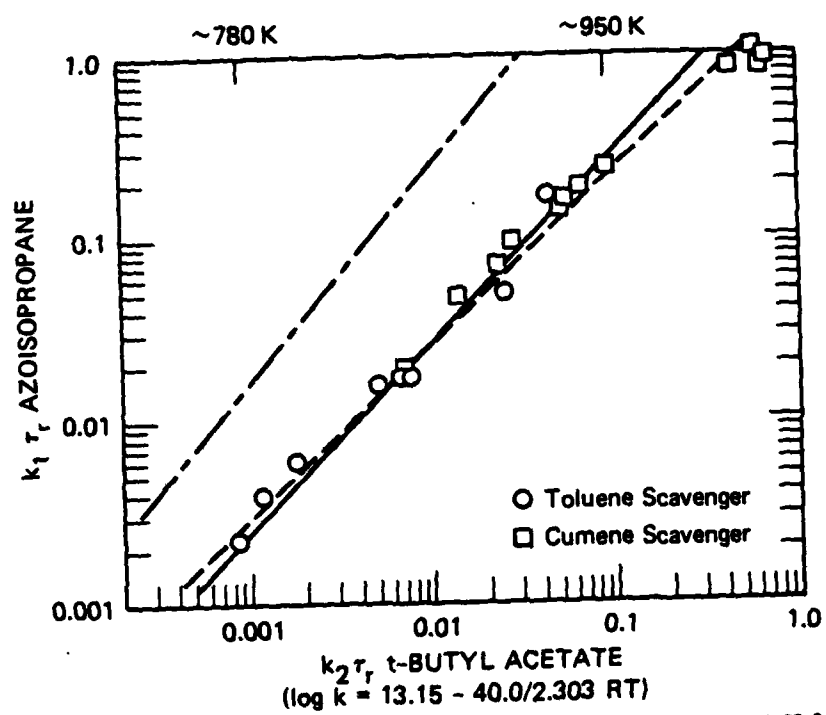


JA-322522-8

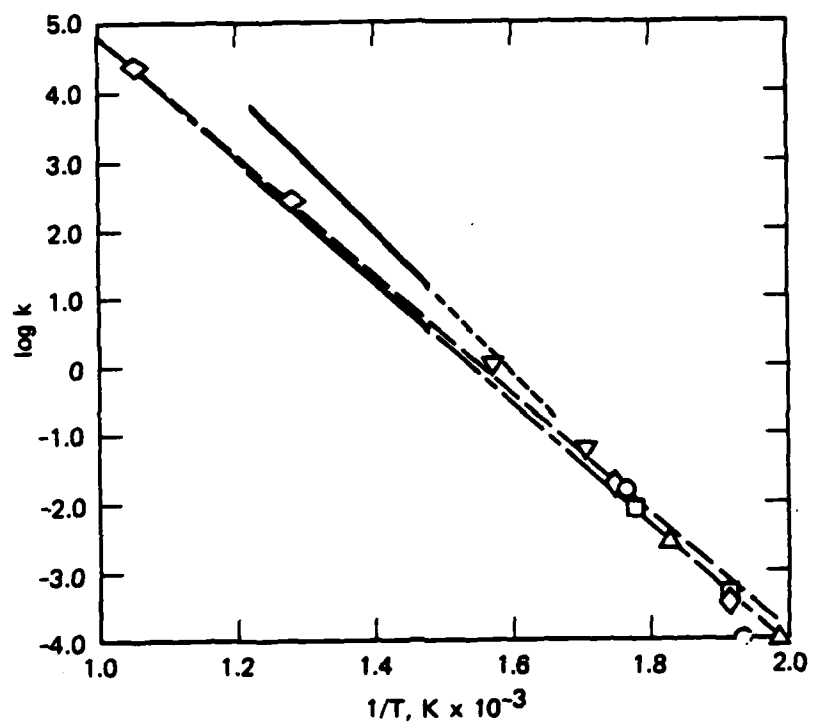


SA-7399-1A





JA-322522-9



JA-322522-10

ATE  
LME  
-8